

## Thermodynamics of multicomponent olivines and the solution properties of $(\text{Ni},\text{Mg},\text{Fe})_2\text{SiO}_4$ and $(\text{Ca},\text{Mg},\text{Fe})_2\text{SiO}_4$ olivines

MARC HIRSCHMANN

Department of Geological Sciences AJ-20, University of Washington, Seattle, Washington 98195, U.S.A.

### ABSTRACT

A general thermodynamic model is developed that describes the mixing properties of minor and trace divalent cations (Ni, Ca, Mn, Co) in ferromagnesian olivines in terms of octahedral site order-disorder and symmetric enthalpies of mixing. Two cases of this model are presented. The first is applicable to true ternary solutions, where minor components (e.g., Ni, Mn, Co) substitute on both octahedral sites, and the second is appropriate for quadrilateral solutions, where substitution is limited to a single site (e.g., Ca on M2). The ternary model is calibrated for Ni-bearing olivines from consideration of site occupancy determinations and heterogeneous exchange equilibria. Ca-bearing olivines are calibrated from consideration of miscibility gaps. Both the models for  $(\text{Ni},\text{Mg},\text{Fe})_2\text{SiO}_4$  and  $(\text{Ca},\text{Mg},\text{Fe})_2\text{SiO}_4$  olivines are internally consistent with Sack and Ghiorso's (1989) analysis of ferromagnesian olivines and with the standard state data base of Berman (1988).

The resulting analysis of the mixing properties of nickel magnesium iron olivines indicates small negative deviations from ideality in Fe-free olivines and greater negative deviations in ferromagnesian olivines. Predictions of Ni-Fe exchange between olivines and FeNi alloys agree with experimentally determined distributions. Predicted mixing properties of calcian olivines on the Ca-poor side of the solvus are similar to those calculated from the formulation of Davidson and Lindsley (1989), but small differences arise from adoption here of a larger Fe-Mg interaction energy.

### INTRODUCTION

Natural ferromagnesian olivines contain minor amounts of additional divalent cations, including Ca, Mn, Ni, and Co. Although concentrations of these elements in olivine are typically small (Ca < 1.0%, Mn < 1.0%, Ni < 4000 ppm, Co < 150 ppm; Simpkin and Smith, 1970; Stosch, 1981), their distribution relative to coexisting phases is of great importance in understanding magmatic and planetary differentiation. Exchange of these elements between olivine and coexisting phases is also used in geothermometry. In view of the many petrologic applications of equilibria involving minor components in olivine, it is necessary to develop a thermodynamic model for multicomponent olivine solutions. Once calibrated, such a model may be used to investigate mass transfer during igneous and planetary evolution and may be combined with thermodynamic treatments of coexisting phases to provide mineral-mineral and mineral-melt geothermometers and geobarometers.

Partitioning of transition metals, particularly Ni, between olivine and silicate liquids is frequently used to interpret and model the petrogenesis of mafic and ultramafic magmas (e.g., Leeman and Lindstrom, 1978; Hart and Davis, 1978; Kinzler et al., 1990). Interpretation of partitioning of transition metals between olivine, molten

silicate, and metallic phases is fundamental to our present understanding of terrestrial core formation (Jones and Drake, 1986), the origin of the Moon (e.g., Ringwood, 1986; Ringwood and Seifert, 1986), and the composition of the lunar core (Seifert et al., 1988). Much of this work is based on empirically determined distribution coefficients (e.g., Leeman and Lindstrom, 1978; Takahashi, 1978; Seifert et al., 1988). These partition coefficients vary with temperature, composition, and to a lesser degree, pressure and  $f_{\text{O}_2}$ , and there have been several recent attempts to predict olivine-liquid partition coefficients based on solution models for silicate liquids (Doyle and Naldrett, 1987; Kinzler et al., 1990) or generalized methods for calculating activities of trace constituents in olivine (Colson et al., 1988, 1989).

The temperature dependence of Ni partitioning between olivine, other mafic minerals, and silicate liquids has led to proposal of several geothermometers. Empirical calibrations have been presented for olivine-clinopyroxene (Hakli and Wright, 1967), olivine-orthopyroxene (Podvin, 1988), and olivine-garnet (Griffen et al., 1989) thermometers. It has also been suggested that partitioning of Ni between olivine and melts could be employed as a geothermometer (Leeman and Lindstrom, 1978), though this requires an effective method for removing the compositional dependence on olivine-melt partitioning.

The distribution of Ca between olivine and coexisting phases, particularly clinopyroxene, is also of petrologic interest. Olivine-liquid exchange of Ca has been proposed as a geothermometer (Jurewicz and Watson, 1988), and Ca exchange between olivine and clinopyroxene is used in geobarometry of ultramafic xenoliths (e.g., Adams and Bishop, 1986). Excellent treatments of the thermodynamics of Ca-bearing olivine solutions have been developed by Davidson and Mukhopadhyay (1984) and Davidson and Lindsley (1989), but recent reconsideration of the properties of ferromagnesian olivines (Sack and Ghiorso, 1989) suggests that recalibration could improve the utility of calcian olivine solution models.

The approach taken in this contribution is to develop a thermodynamic model that incorporates the properties of the pure olivine end-members and recognizes the effect of octahedral site preferences and olivine composition (Mg-Fe content) on the mixing properties of minor substituents. Calibrations are developed for Ni-bearing and Ca-bearing olivines. The models may be combined with available experimental partitioning data to calibrate the solution properties of the components of interest in melts and orthopyroxenes. Resulting paired models may then be incorporated in mass transfer algorithms (Ghiorso, 1985) to predict the behavior of the elements of interest during petrologic processes and applied directly to geothermometry and geobarometry.

### THERMODYNAMIC MODEL

Divalent cations in olivines reside in two nonequivalent octahedral sites, M1 and M2. M1 is slightly smaller (11.8 Å<sup>3</sup> vs. 12.4 Å<sup>3</sup> for M2 in forsterite; Boström, 1987) and less symmetric than M2. Although cation ordering between Mg and Fe is weak (e.g., Motoyama and Matsumoto, 1989), all other divalent cations show pronounced site preferences. Ca and Mn are primarily included in M2 (Brown, 1980); Ni and Co are concentrated in M1 (e.g., Ghose and Wan, 1974; Rajamani et al., 1975). Because cation ordering reduces the configurational entropy of a mineral, it must be accounted for in a thermodynamic model.

The energetics of mineral solutions may be described as a function of composition and ordering state by dividing the Gibbs free energy into contributions from configurational entropy,  $\bar{S}^{\text{ic}}$ , and vibrational Gibbs energy,  $\bar{G}^*$  (Thompson, 1969, 1970):

$$\bar{G} = -T\bar{S}^{\text{ic}} + \bar{G}^* \quad (1)$$

The vibrational Gibbs energy, which is the sum of the standard-state free energies of the pure end-members and all excess mixing energies not accounted for in the configurational entropy, is then expanded with a second-order Taylor series as a function of an appropriate set of compositional and ordering variables (Thompson, 1969, 1970; Sack, 1980; Sack and Ghiorso, 1989). For two-site solutions such as olivines, the Taylor expansion has the general form

$$\bar{G}^* = \bar{G}_0^* + \sum_{i=1}^{2n-2} i\bar{G}_i^* + \sum_{j=1}^{2n-2} \sum_{k=j}^{2n-2} jk\bar{G}_{jk}^* \quad (2)$$

where  $n$  is the number of macroscopically distinguishable solution components;  $i$ ,  $j$ , and  $k$  are indices of  $(n-1)$  compositional and  $(n-1)$  ordering variables; and the subscripted  $\bar{G}^*$ 's coefficients of the Taylor expansion. Truncation of the Taylor expansion after the second degree terms yields four solution parameters for each bounding binary and allows evaluation of between-site ordering energies and symmetric, regular-solution-like mixing energies within and between sites. Including third degree terms in the expansion would allow incorporation of asymmetric mixing energies and other ternary interaction parameters, but calibration of these terms may not be possible from available data.

In theory, the solution properties of natural olivines could be described by a comprehensive model that accounts for substitution and ordering of all relevant divalent cations. Calibration of such a model would, however, require far more experimental data than are likely to be available. As the concentration of components other than forsterite and fayalite is in most cases small, treatment of natural olivines does not require accounting for interactions between nonferromagnesian components. Instead, a series of consistent ternary cases (e.g., Ni-Mg-Fe or Mn-Mg-Fe) of the general model may be derived and calibrated independently but applied simultaneously.

Two cases of the general model are required to account for nonferromagnesian olivine components: (1) a true ternary case in which the third component substitutes on both octahedral sites but may be partially ordered on these sites and (2) a quadrilateral case, in which the third component is generated by substitution on one site only (e.g., Ca on M2 to give CaMgSiO<sub>4</sub>). When two cations are specified in olivine formulas, their order is meant to specify site occupation. The first site specified is M2, followed by M1, e.g., CaMgSiO<sub>4</sub> = Ca<sup>M2</sup>Mg<sup>M1</sup>SiO<sub>4</sub>. In this section, thermodynamic formulations for each case are developed. For convenience, the ternary model is phrased using Ni<sub>2</sub>SiO<sub>4</sub> as the third component.

### Ternary case

Description of ternary solutions requires selection of two linearly independent compositional variables,  $q$  and  $r$ :

$$q = 2X_{\text{Ni}_2\text{SiO}_4}^{\text{Ol}} - 1, \quad r = 2X_{\text{Fe}_2\text{SiO}_4}^{\text{Ol}} - 1. \quad (3a, 3b)$$

The degree of long-range order is described by linear measures of site occupancies,  $s$  and  $t$ :

$$s = X_{\text{Fe}}^{\text{M2}} - X_{\text{Fe}}^{\text{M1}}, \quad t = X_{\text{Ni}}^{\text{M1}} - X_{\text{Ni}}^{\text{M2}} \quad (3c, 3d)$$

where  $X_j^{\text{Mi}}$  represents the molar concentration of element  $j$  on the  $\text{Mi}$ th site. The individual site occupancies in terms of these variables are

$$X_{\text{Ni}}^{\text{M1}} = \frac{q + t + 1}{2}, \quad X_{\text{Ni}}^{\text{M2}} = \frac{q - t + 1}{2} \quad (4a, 4b)$$

$$X_{\text{Fe}}^{\text{M1}} = \frac{r-s+1}{2}, \quad X_{\text{Fe}}^{\text{M2}} = \frac{r+s+1}{2} \quad (4c, 4d)$$

$$X_{\text{Mg}}^{\text{M1}} = \frac{s-q-t-r}{2}, \quad X_{\text{Mg}}^{\text{M2}} = \frac{t-q-r-s}{2} \quad (4e, 4f)$$

and the configurational entropy is given by

$$\begin{aligned} \bar{S}^{\text{ic}} = & -R(X_{\text{Fe}}^{\text{M2}} \ln X_{\text{Fe}}^{\text{M2}} + X_{\text{Fe}}^{\text{M1}} \ln X_{\text{Fe}}^{\text{M1}} + X_{\text{Mg}}^{\text{M2}} \ln X_{\text{Mg}}^{\text{M2}} \\ & + X_{\text{Mg}}^{\text{M1}} \ln X_{\text{Mg}}^{\text{M1}} + X_{\text{Ni}}^{\text{M2}} \ln X_{\text{Ni}}^{\text{M2}} + X_{\text{Ni}}^{\text{M1}} \ln X_{\text{Ni}}^{\text{M1}}). \end{aligned} \quad (5)$$

From Equation 2, the vibrational Gibbs energy is

$$\begin{aligned} \bar{G}^* = & \bar{G}_0^* + \bar{G}_q^* q + \bar{G}_r^* r + \bar{G}_s^* s + \bar{G}_t^* t + \bar{G}_{qr}^* qr \\ & + \bar{G}_{qs}^* qs + \bar{G}_{qt}^* qt + \bar{G}_{rs}^* rs + \bar{G}_{rt}^* rt + \bar{G}_{st}^* st \\ & + \bar{G}_{qq}^* qq + \bar{G}_{rr}^* rr + \bar{G}_{ss}^* ss + \bar{G}_{tt}^* tt. \end{aligned} \quad (6)$$

Calibration and application of this solution model is facilitated by rephrasing the 15 coefficients ( $\bar{G}_{i,j}^*$ ) in Equation 6 in terms of the standard-state free energies of the macroscopic compositional end-members and the solution parameters that describe the excess free energy of mixing more conveniently. Expressions for the coefficients to the vibrational energy expansion are derived by first evaluating Equation 6 for 15 compositions where  $\bar{G}^*$  is easily characterized. These are the nine microscopically distinguishable end-members (three pure components, e.g.,  $\text{Mg}_2\text{SiO}_4$ ; three completely ordered components, e.g.,  $\text{MgNiSiO}_4$ ; and three antiordered components, e.g.,  $\text{NiMgSiO}_4$ ) and the midpoints of binaries joining six of these end-members. The 15 resulting equations are given in Table 1. Note that the vibrational energy along the midpoints between the vertices includes contributions from regular-solution-like mixing energies that arise from substitution of elements on individual sites,  $\bar{W}_{yz}^{\text{M1}}$  and  $\bar{W}_{yz}^{\text{M2}}$ , where the subscripts  $y$  and  $z$  represent unlike divalent cations. Simultaneous solution of the equations in Table 1 yields expressions for the coefficients of the Taylor expansion in terms of the free energy of formation of the nine end-members and the regular-solution-like terms. After the terms for the free energy of the purely ordered and antiordered end-members are eliminated by substituting the energy of ordering,  $\Delta\bar{G}_{\text{EX}}^{\text{yz}} = \bar{G}_{yz\text{SiO}_4}^0 - \bar{G}_{zy\text{SiO}_4}^0$ , and the reciprocal exchange energy,  $\Delta\bar{G}_{\text{X}}^{\text{yz}} = \bar{G}_{yz\text{SiO}_4}^0 + \bar{G}_{zy\text{SiO}_4}^0 - \bar{G}_{y\text{SiO}_4}^0 - \bar{G}_{z\text{SiO}_4}^0$ , the coefficients are given by the equations in Table 2. The reciprocal exchange energy represents the interaction of unlike cations on unlike sites (Wood and Nicholls, 1978). An expression for  $\bar{G}^*$  in terms of the preferred standard state and solution variables is obtained by substituting the equations in Table 2 back into Equation 6.

The condition for homogeneous intracrystalline equilibrium is derived by simultaneously setting the derivatives of the Gibbs energy with respect to the ordering parameters  $s$  and  $t$  to zero, which gives

$$-\frac{1}{2} RT \ln \left( \frac{X_{\text{Mg}}^{\text{M1}} X_{\text{Fe}}^{\text{M2}}}{X_{\text{Mg}}^{\text{M2}} X_{\text{Fe}}^{\text{M1}}} \right) = \left( \frac{\partial \bar{G}^*}{\partial s} \right)_{q,r,t} \quad (7a)$$

$$-\frac{1}{2} RT \ln \left( \frac{X_{\text{Ni}}^{\text{M1}} X_{\text{Mg}}^{\text{M2}}}{X_{\text{Ni}}^{\text{M2}} X_{\text{Mg}}^{\text{M1}}} \right) = \left( \frac{\partial \bar{G}^*}{\partial t} \right)_{q,r,s} \quad (7b)$$

The chemical potentials of the end-members and the exchange potentials are evaluated by application of the Darken equation (Darken and Gurry, 1953; Ghiorso, 1990a):

$$\begin{aligned} \mu_{\text{Ni}_2\text{SiO}_4} = & \bar{G} + (1-q) \left( \frac{\partial \bar{G}}{\partial q} \right)_{r,s,t} - (1+r) \left( \frac{\partial \bar{G}}{\partial r} \right)_{q,s,t} \\ & - s \left( \frac{\partial \bar{G}}{\partial s} \right)_{q,r,t} - t \left( \frac{\partial \bar{G}}{\partial t} \right)_{q,r,s} \end{aligned} \quad (8a)$$

$$\begin{aligned} \mu_{\text{Fe}_2\text{SiO}_4} = & \bar{G} - (1+q) \left( \frac{\partial \bar{G}}{\partial q} \right)_{r,s,t} + (1-r) \left( \frac{\partial \bar{G}}{\partial r} \right)_{q,s,t} \\ & - s \left( \frac{\partial \bar{G}}{\partial s} \right)_{q,r,t} - t \left( \frac{\partial \bar{G}}{\partial t} \right)_{q,r,s} \end{aligned} \quad (8b)$$

$$\begin{aligned} \mu_{\text{Mg}_2\text{SiO}_4} = & \bar{G} - (1+q) \left( \frac{\partial \bar{G}}{\partial q} \right)_{r,s,t} - (1+r) \left( \frac{\partial \bar{G}}{\partial r} \right)_{q,s,t} \\ & - s \left( \frac{\partial \bar{G}}{\partial s} \right)_{q,r,t} - t \left( \frac{\partial \bar{G}}{\partial t} \right)_{q,r,s} \end{aligned} \quad (8c)$$

$$\mu_{\text{NiMg-1}} = \left( \frac{\partial \bar{G}}{\partial q} \right)_{r,s,t} \quad (8d)$$

$$\mu_{\text{NiFe-1}} = \left( \frac{\partial \bar{G}}{\partial q} \right)_{r,s,t} - \left( \frac{\partial \bar{G}}{\partial r} \right)_{q,s,t} \quad (8e)$$

$$\mu_{\text{FeMg-1}} = \left( \frac{\partial \bar{G}}{\partial r} \right)_{q,s,t} \quad (8f)$$

Expressions for the equilibrium ordering state and for exchange chemical potentials are given in Appendix 1.

### Quadrilateral case

Construction of a model appropriate for quadrilateral olivines, where Ca is restricted to the M2 site, necessitates a modification of the general form of the Taylor expansion (Eq. 2). Specifying the location of Ca atoms reduces the degrees of freedom of the solution so that only three variables are required to describe accessible composition-ordering space. Beginning again with the composition and ordering variables  $r$  and  $s$ ,

$$r = 2X_{\text{Fe}_2\text{SiO}_4}^{\text{O1}} - 1, \quad s = X_{\text{Fe}}^{\text{M2}} - X_{\text{Fe}}^{\text{M1}} \quad (3b, 3c)$$

an additional compositional variable,  $p$ , is defined:

$$p = 2X_{\text{Ca}}^{\text{O1}}. \quad (9)$$

Site mole fractions phrased in terms of  $p$ ,  $r$ , and  $s$  are

$$X_{\text{Fe}}^{\text{M1}} = \frac{(r-s+1)}{2}, \quad X_{\text{Fe}}^{\text{M2}} = \frac{(r+s+1)}{2} \quad (10a, 10b)$$

$$X_{\text{Mg}}^{\text{M1}} = \frac{(s-r+1)}{2} \quad (10c)$$

$$X_{\text{Mg}}^{\text{M2}} = \frac{(1-r-s-2p)}{2}, \quad X_{\text{Ca}}^{\text{M2}} = p. \quad (10d, 10e)$$

TABLE 1. Vibrational Gibbs energy evaluated at end-members and midpoints of binaries for nickel magnesium iron olivines

$$\begin{aligned}
 \bar{G}_{\text{FeFeSiO}_4}^0 &= \bar{G}_0^* - \bar{G}_r^* + \bar{G}_i^* - \bar{G}_{gr}^* + \bar{G}_{qs}^* + \bar{G}_{rs}^* \\
 \bar{G}_{\text{MgMgSiO}_4}^0 &= \bar{G}_0^* - \bar{G}_r^* - \bar{G}_i^* + \bar{G}_{gr}^* + \bar{G}_{qs}^* + \bar{G}_{rs}^* \\
 \bar{G}_{\text{NiSiO}_4}^0 &= \bar{G}_0^* + \bar{G}_r^* - \bar{G}_i^* - \bar{G}_{gr}^* + \bar{G}_{qs}^* + \bar{G}_{rs}^* \\
 \bar{G}_{\text{FeMgSiO}_4}^0 &= \bar{G}_0^* - \bar{G}_r^* - \bar{G}_i^* + \bar{G}_{gr}^* + \bar{G}_{qs}^* + \bar{G}_{rs}^* \\
 \bar{G}_{\text{MgFeSiO}_4}^0 &= \bar{G}_0^* - \bar{G}_r^* - \bar{G}_i^* + \bar{G}_{gr}^* + \bar{G}_{qs}^* + \bar{G}_{rs}^* \\
 \bar{G}_{\text{FeNiSiO}_4}^0 &= \bar{G}_0^* + \bar{G}_r^* + \bar{G}_i^* + \bar{G}_{gr}^* + \bar{G}_{qs}^* + \bar{G}_{rs}^* \\
 \bar{G}_{\text{NiFeSiO}_4}^0 &= \bar{G}_0^* - \bar{G}_r^* - \bar{G}_i^* + \bar{G}_{gr}^* + \bar{G}_{qs}^* + \bar{G}_{rs}^* \\
 \bar{G}_{\text{MgNiSiO}_4}^0 &= \bar{G}_0^* - \bar{G}_r^* + \bar{G}_i^* - \bar{G}_{gr}^* + \bar{G}_{qs}^* + \bar{G}_{rs}^* \\
 \bar{G}_{\text{NiMgSiO}_4}^0 &= \bar{G}_0^* - \bar{G}_r^* - \bar{G}_i^* + \bar{G}_{gr}^* + \bar{G}_{qs}^* + \bar{G}_{rs}^* \\
 1/2 \bar{G}_{\text{CaMgSiO}_4}^0 + 1/2 \bar{G}_{\text{MgMgSiO}_4}^0 + 1/4 W_{\text{CaMg}}^{M2} &= \bar{G}_0^* - 1/2 \bar{G}_r^* - \bar{G}_i^* - 1/2 \bar{G}_{gr}^* + 1/2 \bar{G}_{qs}^* + 1/2 \bar{G}_{rs}^* \\
 &\quad + 1/4 \bar{G}_{gr}^* + 1/2 \bar{G}_{qs}^* + \bar{G}_{rs}^* + 1/4 \bar{G}_{rs}^* \\
 1/2 \bar{G}_{\text{MgMgSiO}_4}^0 + 1/2 \bar{G}_{\text{NiMgSiO}_4}^0 + 1/4 W_{\text{NiMg}}^{M2} &= \bar{G}_0^* - 1/2 \bar{G}_r^* - \bar{G}_i^* + 1/2 \bar{G}_{gr}^* + 1/2 \bar{G}_{qs}^* \\
 &\quad - 1/4 \bar{G}_{gr}^* - 1/2 \bar{G}_{qs}^* + 1/4 \bar{G}_{rs}^* + \bar{G}_{rs}^* + 1/4 \bar{G}_{rs}^* \\
 1/2 \bar{G}_{\text{FeFeSiO}_4}^0 + 1/2 \bar{G}_{\text{NiFeSiO}_4}^0 + 1/4 W_{\text{FeNi}}^{M2} &= \bar{G}_0^* - 1/2 \bar{G}_r^* + 1/2 \bar{G}_{gr}^* - 1/2 \bar{G}_{qs}^* - 1/2 \bar{G}_{rs}^* \\
 &\quad - 1/4 \bar{G}_{gr}^* + 1/4 \bar{G}_{qs}^* + 1/4 \bar{G}_{rs}^* - 1/4 \bar{G}_{rs}^* - 1/4 \bar{G}_{rs}^* + 1/4 \bar{G}_{rs}^* + 1/4 \bar{G}_{rs}^* + 1/4 \bar{G}_{rs}^* \\
 &\quad + 1/4 \bar{G}_{rs}^* + 1/4 \bar{G}_{rs}^* + 1/4 \bar{G}_{rs}^* \\
 1/2 \bar{G}_{\text{FeFeSiO}_4}^0 + 1/2 \bar{G}_{\text{FeNiSiO}_4}^0 + 1/4 W_{\text{FeNi}}^{M1} &= \bar{G}_0^* - 1/2 \bar{G}_r^* + 1/2 \bar{G}_{gr}^* + 1/2 \bar{G}_{qs}^* + 1/2 \bar{G}_{rs}^* \\
 &\quad - 1/4 \bar{G}_{gr}^* - 1/4 \bar{G}_{qs}^* - 1/4 \bar{G}_{rs}^* + 1/4 \bar{G}_{rs}^* + 1/4 \bar{G}_{rs}^* + 1/4 \bar{G}_{rs}^* + 1/4 \bar{G}_{rs}^* + 1/4 \bar{G}_{rs}^* \\
 &\quad + 1/4 \bar{G}_{rs}^* + 1/4 \bar{G}_{rs}^* + 1/4 \bar{G}_{rs}^* \\
 1/2 \bar{G}_{\text{FeFeSiO}_4}^0 + 1/2 \bar{G}_{\text{MgFeSiO}_4}^0 + 1/4 W_{\text{FeMg}}^{M2} &= \bar{G}_0^* - \bar{G}_r^* + 1/2 \bar{G}_{gr}^* - 1/2 \bar{G}_{qs}^* - 1/2 \bar{G}_{rs}^* \\
 &\quad + 1/2 \bar{G}_{qs}^* - 1/4 \bar{G}_{rs}^* + \bar{G}_{rs}^* + 1/4 \bar{G}_{rs}^* + 1/4 \bar{G}_{rs}^* \\
 1/2 \bar{G}_{\text{FeFeSiO}_4}^0 + 1/2 \bar{G}_{\text{MgMgSiO}_4}^0 + 1/4 W_{\text{FeMg}}^{M1} &= \bar{G}_0^* - \bar{G}_r^* + 1/2 \bar{G}_{gr}^* + 1/2 \bar{G}_{qs}^* - 1/2 \bar{G}_{rs}^* \\
 &\quad - 1/2 \bar{G}_{gr}^* + 1/4 \bar{G}_{qs}^* + \bar{G}_{rs}^* + 1/4 \bar{G}_{rs}^* + 1/4 \bar{G}_{rs}^*
 \end{aligned}$$

Proceeding as before, the configurational entropy is

$$\begin{aligned}
 S^{\text{TC}} &= -R(X_{\text{Ca}}^{M2} \ln X_{\text{Ca}}^{M2} + X_{\text{Mg}}^{M2} \ln X_{\text{Mg}}^{M2} + X_{\text{Fe}}^{M1} \ln X_{\text{Fe}}^{M1} \\
 &\quad + X_{\text{Mg}}^{M2} \ln X_{\text{Mg}}^{M2} + X_{\text{Mg}}^{M1} \ln X_{\text{Mg}}^{M1}) \quad (11)
 \end{aligned}$$

and the expansion of the vibrational Gibbs energy is

$$\begin{aligned}
 \bar{G}^* &= \bar{G}_0^* + \bar{G}_p^* p + \bar{G}_r^* r + \bar{G}_i^* s + \bar{G}_{pr}^* pr + \bar{G}_{ps}^* ps \\
 &\quad + \bar{G}_{rs}^* rs + \bar{G}_{pp}^* pp + \bar{G}_{rr}^* rr + \bar{G}_{ss}^* ss. \quad (12)
 \end{aligned}$$

The coefficients of the expansion are solved in a manner analogous to that used above. Expressions for  $\bar{G}^*$  evaluated at the end-members and midpoints of composition-ordering space are given in Table 3; solutions for the coefficients of the Taylor expansion are given in Table 4 in terms of the preferred set of variables,  $\Delta \bar{G}_{\text{EX}}^{\text{FeMg}}$ ,  $\Delta \bar{G}_{\text{X}}^{\text{FeMg}}$ ,

TABLE 2. Coefficients of Taylor expansion of vibrational Gibbs energy for nickel magnesium iron olivines

$$\begin{aligned}
 \bar{G}_0^* &= 1/4[2\bar{G}_{\text{Fe}_2\text{SiO}_4}^0 + 2\bar{G}_{\text{Fe}_2\text{SiO}_4}^0 + (\Delta \bar{G}_{\text{X}}^{\text{FeNi}} + W_{\text{FeNi}}^{M2} + W_{\text{FeNi}}^{M1}) \\
 \bar{G}_r^* &= 1/4[2\bar{G}_{\text{Mg}_2\text{SiO}_4}^0 - 2\bar{G}_{\text{Mg}_2\text{SiO}_4}^0 + (\Delta \bar{G}_{\text{X}}^{\text{FeNi}} + W_{\text{FeNi}}^{M2} + W_{\text{FeNi}}^{M1}) - (\Delta \bar{G}_{\text{X}}^{\text{MgNi}} + \\
 &\quad W_{\text{MgNi}}^{M2} + W_{\text{MgNi}}^{M1}) - (\Delta \bar{G}_{\text{X}}^{\text{FeMg}} + W_{\text{FeMg}}^{M2} + W_{\text{FeMg}}^{M1})] \\
 \bar{G}_i^* &= 1/4[2\bar{G}_{\text{Fe}_2\text{SiO}_4}^0 - 2\bar{G}_{\text{Mg}_2\text{SiO}_4}^0 + (\Delta \bar{G}_{\text{X}}^{\text{FeNi}} + W_{\text{FeNi}}^{M2} + W_{\text{FeNi}}^{M1}) - (\Delta \bar{G}_{\text{X}}^{\text{MgNi}} + \\
 &\quad W_{\text{MgNi}}^{M2} + W_{\text{MgNi}}^{M1}) - (\Delta \bar{G}_{\text{X}}^{\text{FeMg}} + W_{\text{FeMg}}^{M2} + W_{\text{FeMg}}^{M1})] \\
 \bar{G}_s^* &= 1/4[(\Delta \bar{G}_{\text{EX}}^{\text{FeNi}} - W_{\text{FeNi}}^{M1} + W_{\text{FeNi}}^{M2}) - (\Delta \bar{G}_{\text{EX}}^{\text{MgNi}} - W_{\text{MgNi}}^{M1} + W_{\text{MgNi}}^{M2}) + \\
 &\quad (\Delta \bar{G}_{\text{EX}}^{\text{FeMg}} + W_{\text{FeMg}}^{M1} - W_{\text{FeMg}}^{M2})] \\
 \bar{G}_{gr}^* &= 1/4[(\Delta \bar{G}_{\text{EX}}^{\text{FeNi}} + W_{\text{FeNi}}^{M1} - W_{\text{FeNi}}^{M2}) + (\Delta \bar{G}_{\text{EX}}^{\text{MgNi}} - W_{\text{MgNi}}^{M1} + W_{\text{MgNi}}^{M2}) - \\
 &\quad (\Delta \bar{G}_{\text{EX}}^{\text{FeMg}} + W_{\text{FeMg}}^{M1} - W_{\text{FeMg}}^{M2})] \\
 \bar{G}_{qs}^* &= 1/4[(\Delta \bar{G}_{\text{EX}}^{\text{FeNi}} + W_{\text{FeNi}}^{M1} + W_{\text{FeNi}}^{M2}) - (\Delta \bar{G}_{\text{EX}}^{\text{MgNi}} + W_{\text{MgNi}}^{M1} + W_{\text{MgNi}}^{M2}) - \\
 &\quad (\Delta \bar{G}_{\text{EX}}^{\text{FeMg}} + W_{\text{FeMg}}^{M1} + W_{\text{FeMg}}^{M2})] \\
 \bar{G}_{rs}^* &= 1/4[(\Delta \bar{G}_{\text{EX}}^{\text{FeNi}} - W_{\text{FeNi}}^{M1} + W_{\text{FeNi}}^{M2}) - (\Delta \bar{G}_{\text{EX}}^{\text{MgNi}} - W_{\text{MgNi}}^{M1} + W_{\text{MgNi}}^{M2}) - \\
 &\quad (\Delta \bar{G}_{\text{EX}}^{\text{FeMg}} - W_{\text{FeMg}}^{M1} + W_{\text{FeMg}}^{M2})] \\
 \bar{G}_{gr}^* &= 1/2(W_{\text{MgNi}}^{M2} - W_{\text{MgNi}}^{M1}) \\
 \bar{G}_{qs}^* &= 1/2(W_{\text{FeNi}}^{M1} - W_{\text{FeNi}}^{M2}) \\
 \bar{G}_{rs}^* &= 1/4[(\Delta \bar{G}_{\text{EX}}^{\text{FeNi}} + W_{\text{FeNi}}^{M1} - W_{\text{FeNi}}^{M2}) - (\Delta \bar{G}_{\text{EX}}^{\text{MgNi}} + W_{\text{MgNi}}^{M1} - W_{\text{MgNi}}^{M2}) - \\
 &\quad (\Delta \bar{G}_{\text{EX}}^{\text{FeMg}} + W_{\text{FeMg}}^{M1} - W_{\text{FeMg}}^{M2})] \\
 \bar{G}_{gr}^* &= 1/4[(\Delta \bar{G}_{\text{EX}}^{\text{FeNi}} - W_{\text{FeNi}}^{M1} - W_{\text{FeNi}}^{M2}) - (\Delta \bar{G}_{\text{EX}}^{\text{MgNi}} - W_{\text{MgNi}}^{M1} - W_{\text{MgNi}}^{M2}) - \\
 &\quad (\Delta \bar{G}_{\text{EX}}^{\text{FeMg}} - W_{\text{FeMg}}^{M1} - W_{\text{FeMg}}^{M2})] \\
 \bar{G}_{qs}^* &= 1/4[(\Delta \bar{G}_{\text{EX}}^{\text{FeNi}} + W_{\text{FeNi}}^{M1} + W_{\text{FeNi}}^{M2}) - (\Delta \bar{G}_{\text{EX}}^{\text{MgNi}} + W_{\text{MgNi}}^{M1} + W_{\text{MgNi}}^{M2}) + \\
 &\quad (\Delta \bar{G}_{\text{EX}}^{\text{FeMg}} + W_{\text{FeMg}}^{M1} + W_{\text{FeMg}}^{M2})] \\
 \bar{G}_{rs}^* &= 1/4[(\Delta \bar{G}_{\text{EX}}^{\text{FeNi}} - W_{\text{FeNi}}^{M1} - W_{\text{FeNi}}^{M2}) - (\Delta \bar{G}_{\text{EX}}^{\text{MgNi}} - W_{\text{MgNi}}^{M1} - W_{\text{MgNi}}^{M2}) + \\
 &\quad (\Delta \bar{G}_{\text{EX}}^{\text{FeMg}} - W_{\text{FeMg}}^{M1} - W_{\text{FeMg}}^{M2})] \\
 \bar{G}_{gr}^* &= 1/4[(\Delta \bar{G}_{\text{EX}}^{\text{FeNi}} + W_{\text{FeNi}}^{M1} + W_{\text{FeNi}}^{M2}) - (\Delta \bar{G}_{\text{EX}}^{\text{MgNi}} + W_{\text{MgNi}}^{M1} + W_{\text{MgNi}}^{M2}) - \\
 &\quad (\Delta \bar{G}_{\text{EX}}^{\text{FeMg}} + W_{\text{FeMg}}^{M1} + W_{\text{FeMg}}^{M2})] \\
 \bar{G}_{qs}^* &= 1/4[(\Delta \bar{G}_{\text{EX}}^{\text{FeNi}} - W_{\text{FeNi}}^{M1} - W_{\text{FeNi}}^{M2}) - (\Delta \bar{G}_{\text{EX}}^{\text{MgNi}} - W_{\text{MgNi}}^{M1} - W_{\text{MgNi}}^{M2}) + \\
 &\quad (\Delta \bar{G}_{\text{EX}}^{\text{FeMg}} - W_{\text{FeMg}}^{M1} - W_{\text{FeMg}}^{M2})] \\
 \bar{G}_{rs}^* &= 1/4[(\Delta \bar{G}_{\text{EX}}^{\text{FeNi}} + W_{\text{FeNi}}^{M1} + W_{\text{FeNi}}^{M2}) - (\Delta \bar{G}_{\text{EX}}^{\text{MgNi}} + W_{\text{MgNi}}^{M1} + W_{\text{MgNi}}^{M2}) + \\
 &\quad (\Delta \bar{G}_{\text{EX}}^{\text{FeMg}} + W_{\text{FeMg}}^{M1} + W_{\text{FeMg}}^{M2})]
 \end{aligned}$$

TABLE 3. Vibrational Gibbs energy evaluated at end-members and midpoints of binaries for calcium magnesium iron olivines

$$\begin{aligned}
 \bar{G}_{\text{CaMgSiO}_4}^0 &= \bar{G}_0^* + \bar{G}_p^* - \bar{G}_r^* - \bar{G}_{pr}^* + \bar{G}_{ps}^* + \bar{G}_{rs}^* \\
 \bar{G}_{\text{CaFeSiO}_4}^0 &= \bar{G}_0^* + \bar{G}_p^* - \bar{G}_r^* - \bar{G}_{pr}^* + \bar{G}_{ps}^* + \bar{G}_{rs}^* \\
 \bar{G}_{\text{MgMgSiO}_4}^0 &= \bar{G}_0^* - \bar{G}_r^* + \bar{G}_{rs}^* \\
 \bar{G}_{\text{FeFeSiO}_4}^0 &= \bar{G}_0^* + \bar{G}_r^* + \bar{G}_{rs}^* \\
 \bar{G}_{\text{MgFeSiO}_4}^0 &= \bar{G}_0^* - \bar{G}_r^* + \bar{G}_{rs}^* \\
 \bar{G}_{\text{CaMgSiO}_4}^0 + 1/2 \bar{G}_{\text{MgMgSiO}_4}^0 + 1/4 W_{\text{CaMg}}^{M2} &= \bar{G}_0^* + 1/2 \bar{G}_p^* - \bar{G}_r^* - 1/2 \bar{G}_{pr}^* + \\
 &\quad 1/4 \bar{G}_{ps}^* + \bar{G}_{rs}^* \\
 1/2 \bar{G}_{\text{CaFeSiO}_4}^0 + 1/2 \bar{G}_{\text{FeFeSiO}_4}^0 + 1/4 W_{\text{CaFe}}^{M2} &= \bar{G}_0^* + 1/2 \bar{G}_p^* + 1/2 \bar{G}_r^* - 1/2 \bar{G}_{pr}^* + \\
 &\quad 1/4 \bar{G}_{ps}^* - 1/4 \bar{G}_{rs}^* - 1/4 \bar{G}_{rs}^* + 1/4 \bar{G}_{rs}^* + \\
 &\quad 1/4 \bar{G}_{rs}^* + 1/4 \bar{G}_{rs}^* \\
 1/2 \bar{G}_{\text{FeFeSiO}_4}^0 + 1/2 \bar{G}_{\text{MgMgSiO}_4}^0 + 1/4 W_{\text{FeMg}}^{M1} &= \bar{G}_0^* + 1/2 \bar{G}_p^* + 1/2 \bar{G}_r^* + 1/2 \bar{G}_{rs}^* + \\
 &\quad 1/4 \bar{G}_{rs}^* + 1/4 \bar{G}_{rs}^* \\
 1/2 \bar{G}_{\text{FeFeSiO}_4}^0 + 1/2 \bar{G}_{\text{MgFeSiO}_4}^0 + 1/4 W_{\text{FeMg}}^{M2} &= \bar{G}_0^* + 1/2 \bar{G}_p^* - 1/2 \bar{G}_{pr}^* - 1/2 \bar{G}_{rs}^* + \\
 &\quad 1/4 \bar{G}_{ps}^* + 1/2 \bar{G}_{rs}^*
 \end{aligned}$$

and  $\bar{F}^0$ , where  $\bar{F}^0$  is the departure from coplanarity of the Gibbs energy of the four end-members:

$$\bar{F}^0 = 2(\bar{G}_{\text{CaMgSiO}_4}^0 - \bar{G}_{\text{CaFeSiO}_4}^0) + \bar{G}_{\text{Fe}_2\text{SiO}_4}^0 - \bar{G}_{\text{Mg}_2\text{SiO}_4}^0 \quad (13)$$

(Davidson and Mukhopadhyay, 1984; Davidson, 1985).

The equilibrium ordering state is given by

$$-\frac{1}{2} RT \ln \left( \frac{X_{\text{Mg}}^{M1} X_{\text{Fe}}^{M2}}{X_{\text{Mg}}^{M2} X_{\text{Fe}}^{M1}} \right) = \left( \frac{\partial \bar{G}^*}{\partial s} \right)_{p,r} \quad (14)$$

and the chemical potentials of end-members and exchange operators by

$$\begin{aligned}
 \mu_{\text{CaMgSiO}_4} &= \bar{G} + (1 - p) \left( \frac{\partial \bar{G}}{\partial p} \right)_{r,s} \\
 &\quad - (1 + r) \left( \frac{\partial \bar{G}}{\partial r} \right)_{p,r} - s \left( \frac{\partial \bar{G}}{\partial s} \right)_{p,r} \quad (15a)
 \end{aligned}$$

$$\begin{aligned}
 \mu_{\text{CaFeSiO}_4} &= \bar{G} + (1 - p) \left( \frac{\partial \bar{G}}{\partial p} \right)_{r,s} \\
 &\quad - r \left( \frac{\partial \bar{G}}{\partial r} \right)_{p,r} - (1 + s) \left( \frac{\partial \bar{G}}{\partial s} \right)_{p,r} \quad (15b)
 \end{aligned}$$

$$\begin{aligned}
 \mu_{\text{Mg}_2\text{SiO}_4} &= \bar{G} - p \left( \frac{\partial \bar{G}}{\partial p} \right)_{r,s} \\
 &\quad - (1 + r) \left( \frac{\partial \bar{G}}{\partial r} \right)_{p,s} - s \left( \frac{\partial \bar{G}}{\partial s} \right)_{p,r} \quad (15c)
 \end{aligned}$$

TABLE 4. Coefficients of Taylor expansion of vibrational Gibbs energy for calcium magnesium iron olivines

$$\begin{aligned}
 \bar{G}_0^* &= 1/2 \bar{G}_{\text{Mg}_2\text{SiO}_4}^0 + 1/2 \bar{G}_{\text{Fe}_2\text{SiO}_4}^0 + 1/4 (\Delta \bar{G}_{\text{X}}^{\text{FeMg}} + W_{\text{FeMg}}^{M1} + W_{\text{FeMg}}^{M2}) \\
 \bar{G}_p^* &= \bar{G}_{\text{CaMgSiO}_4}^0 - \bar{G}_{\text{Mg}_2\text{SiO}_4}^0 + 1/4 (-\bar{F}^0 + \Delta \bar{G}_{\text{EX}}^{\text{FeMg}} - \Delta \bar{G}_{\text{X}}^{\text{FeMg}}) + 1/2 (W_{\text{CaMg}}^{M2} + \\
 &\quad W_{\text{CaMg}}^{M2} - W_{\text{FeMg}}^{M2}) \\
 \bar{G}_r^* &= 1/2 \bar{G}_{\text{Fe}_2\text{SiO}_4}^0 - 1/2 \bar{G}_{\text{Mg}_2\text{SiO}_4}^0 \\
 \bar{G}_s^* &= 1/2 \Delta \bar{G}_{\text{EX}}^{\text{FeMg}} \\
 \bar{G}_{gr}^* &= 1/4 (-\bar{F}^0 + \Delta \bar{G}_{\text{EX}}^{\text{FeMg}} - \Delta \bar{G}_{\text{X}}^{\text{FeMg}}) + 1/2 (W_{\text{CaFe}}^{M2} - W_{\text{CaMg}}^{M2} - W_{\text{FeMg}}^{M2}) \\
 \bar{G}_{qs}^* &= 1/4 (-\bar{F}^0 - \Delta \bar{G}_{\text{EX}}^{\text{FeMg}} + \Delta \bar{G}_{\text{X}}^{\text{FeMg}}) + 1/2 (W_{\text{CaFe}}^{M2} - W_{\text{CaMg}}^{M2} - W_{\text{FeMg}}^{M2}) \\
 \bar{G}_{rs}^* &= 1/2 (W_{\text{FeMg}}^{M1} - W_{\text{FeMg}}^{M2}) \\
 \bar{G}_{gr}^* &= -W_{\text{CaMg}}^{M2} \\
 \bar{G}_{qs}^* &= -1/4 (\Delta \bar{G}_{\text{EX}}^{\text{FeMg}} + W_{\text{FeMg}}^{M1} + W_{\text{FeMg}}^{M2}) \\
 \bar{G}_{rs}^* &= 1/4 (\Delta \bar{G}_{\text{EX}}^{\text{FeMg}} - W_{\text{FeMg}}^{M1} - W_{\text{FeMg}}^{M2})
 \end{aligned}$$

TABLE 5. Standard state properties of Ni<sub>2</sub>SiO<sub>4</sub>

Reference state*		Heat capacity**	
$\bar{H}_f^\circ$	$-1395.3 \pm 2.0$ kJ/mol†	$k_0$	214.997
$\bar{S}^\circ$	$128.1 \pm 0.2$ J/K mol‡	$k_1 \times 10^{-2}$	-10.3075
$\bar{V}$	$4.259 \pm 0.003$ J/bar mol§	$k_2 \times 10^{-6}$	-49.4453
		$k_3 \times 10^{-7}$	62.3705
$V/V^\circ = 28.422 \times 10^{-6} (T - T_r) + 34.355 \times 10^{-10} (T - T_r)^2 - 6.71 \times 10^{-7} (P - P_r)_{  }$			

\* Reference state is 298.15 K and 1 bar.  
\*\*  $C_p = k_0 + k_1 T^{-0.5} + k_2 T^{-2} + k_3 T^{-3}$ . See text.  
† See text.  
‡ Robie et al. (1984).  
§ Evaluated from the mean of lattice parameter determinations by Matsui and Syono (1968), Ozima (1976), Lager and Meagher (1978), Brown (1980), and Boström (1987).  
|| Thermal expansion from regression of lattice parameter determinations up to 1389 K by Lager and Meagher (1978) and Vokurka and Reider (1987). Compressibility from Bass et al. (1984).

$$\mu_{\text{Fe}_2\text{SiO}_4} = \bar{G} - p \left( \frac{\partial \bar{G}}{\partial p} \right)_{r,s} + (1-r) \left( \frac{\partial \bar{G}}{\partial r} \right)_{p,s} - s \left( \frac{\partial \bar{G}}{\partial s} \right)_{p,r} \quad (15d)$$

$$\mu_{\text{MgFe}_{-1}} = - \left( \frac{\partial \bar{G}}{\partial r} \right)_{p,s} \quad (15e)$$

Expressions for the equilibrium ordering state, chemical potentials for calcian olivines (Eqs. 15a, 15b), and Mg-Fe exchange potential (Eq. 15e) are given in Appendix 1.

The resulting model for calcian olivines is similar in spirit and mathematically equivalent to that of Davidson and Mukhopadhyay (1984). However, this model allows for nonideal mixing between Mg and Fe on octahedral sites, and its notation is consistent with that of Sack and Ghiorso (1989).

### STANDARD STATE PROPERTIES

Thermodynamic properties of pure forsterite, fayalite, and monticellite (CaMgSiO<sub>4</sub>) are taken from the internally consistent compilation of Berman (1988). The thermodynamic properties of Ni<sub>2</sub>SiO<sub>4</sub> have been refined from the literature as described below.

The entropy of Ni<sub>2</sub>SiO<sub>4</sub> (Table 5) is from integration of heat capacities determined by adiabatic calorimetry between 5 and 298.15 K and includes the contribution from the antiferromagnetic-paramagnetic transition at 29.15 K (Robie et al., 1984). The heat capacity of Ni<sub>2</sub>SiO<sub>4</sub> above 298.15 K is taken from adiabatic calorimetry (298.15–387 K) and differential scanning calorimetry (DSC) (360–1000 K) measurements of Robie et al. (1984). Because the polynomial fit to these data presented by Robie et al. (1984) goes through a maximum near 1500 K, measured heat capacities are refitted using the procedures and weighting methods recommended by Berman and Brown (1985). The new fit (Table 5) predicts measured heat capacities with an average uncertainty of 0.45% and agrees with the high-temperature theoretical limit calculated from  $C_p = 3nR + \alpha^2 \bar{V}T/\beta$ .

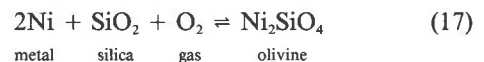
Given these values for entropy and heat capacity, the enthalpy of formation may be determined by noting that Ni<sub>2</sub>SiO<sub>4</sub> decomposes at  $1820 \pm 5$  K to NiO and cristobalite (Phillips et al., 1963; O'Neill, 1987). Using the free energy of formation for NiO (Hemingway, 1990) and the standard-state data for cristobalite from Berman (1988), the enthalpy of formation  $\Delta \bar{H}_f^\circ$  from the elements at the reference temperature, 298.15 K, is  $-1395.3$  kJ.

Navrotsky (1971) measured a change in enthalpy,  $\Delta \bar{H}_f^\circ$ , of  $-13.9 \pm 1.9$  kJ for the reaction



at 965 K using molten salt calorimetry. Integrating down to 298.15 K and accounting for the enthalpy of formation of NiO (Hemingway, 1990) and quartz (Berman, 1988) yields  $-1393.2 \pm 2.9$  kJ for the enthalpy of formation of Ni<sub>2</sub>SiO<sub>4</sub>, in reasonable agreement with that calculated from the decomposition temperature. The adopted enthalpy of formation is  $-1395.3$  kJ, with an estimated uncertainty of 2 kJ (Table 5).

The chosen values of the thermodynamic properties of Ni<sub>2</sub>SiO<sub>4</sub> may be evaluated by comparing experimental determinations of  $\Delta \bar{G}_r$ , the free energy for the reaction



to  $\Delta \bar{G}_r$ , calculated from the parameters for Ni<sub>2</sub>SiO<sub>4</sub> described above and the properties of Ni, O<sub>2</sub>, and silica minerals from Mah and Pankratz (1976), JANAF (Chase et al., 1974), and Berman (1988), respectively (Fig. 1). There is excellent agreement between  $\Delta \bar{G}_r$  for Reaction 17 calculated in this way and the emf studies of Levitskii et al. (1975) and Boström and Rosén (1988). The emf determinations of O'Neill (1987) also agree with calculated free energies between 825 and 1145 °C but diverge below 825 °C. Gas mixing experiments by Campbell and Roeder (1968) and emf determinations by Ottonello and Morlotti (1987) and Taylor and Schmalzried (1964) show considerable scatter. The results of the former two studies are in general agreement with the present calculations, but those of the latter disagree by 2–8 kJ (Fig. 1). The emf determinations of the free energy change for the reaction



between 700 and 1100 °C (Rog and Borchardt, 1984) also agree with those calculated for this reaction, within experimental uncertainty (Fig. 1).

### CALIBRATION

In this section, the mixing properties of Ni- and Ca-bearing olivines are calibrated. The qualitative differences between the various types of data that we seek (e.g., site occupancies, exchange equilibria, and activity-composition measurements) prevent fitting the parameters of

TABLE 6. Solution properties of nickel magnesium iron olivines

yz	MgNi and FeNi*	FeMg
$\Delta H_{yz}^0$	$-12.5 \pm 2.5$ kJ	0.0 kJ**
$\Delta H_{yz}^0 - 2W_{yz}^{O_2}$	$-13.0 \pm 3.0$ kJ	0.0 kJ** †
$\Delta H_{yz}^0 + 2W_{yz}^{O_2}$	$2.2 \pm 0.5$ kJ	$20.3 \pm 0.5$ kJ**
$\Delta V_{yz}^0$	$0.035 \pm 0.012$ J/bar	0.0 J/bar**
$\Delta V_{yz}^0 + 2W_{yz}^V$	$0.01 \pm 0.01$ J/bar	0.030 J/bar**

\* Mg-Ni and Fe-Ni interactions are assumed to be equal (see text).

\*\* Sack and Ghiorso (1989).

† Sack and Ghiorso do not specify a value for  $\Delta H_{yz}^0 - 2W_{yz}^{O_2}$ , but their assumption of zero ordering for iron magnesium olivines is consistent with setting this term equal to zero.

the solution models by simultaneous mathematical optimization. The philosophy adopted is that, given the constraints imposed by the accepted end-member standard state properties, the calibrated solution models should be consistent with as much of the experimental evidence from heterogeneous and homogeneous (intracrystalline) equilibria as possible.

Because it is assumed that explicit recognition of the effects of cation ordering in calculation of the configurational entropy gives an adequate approximation of the entropy of mixing (Bragg and Williams, 1934), no excess entropies are necessary. All terms used to describe the vibrational Gibbs energy except, of course, the free energies of the pure end-members ( $G_{Mg_2SiO_4}^0$ ,  $G_{Fe_2SiO_4}^0$ , etc.) are assumed to have only enthalpic contributions. For example,  $W_{MgNi}^S = 0$ ,  $W_{MgNi}^H = W_{MgNi}^H$ ;  $\Delta S_{MgNi}^0 = 0$ ,  $\Delta G_{MgNi}^0 = \Delta H_{MgNi}^0$ ; and so on.

The analysis of Sack and Ghiorso (1989) demonstrates that adoption of internally consistent standard-state properties of end-members (Berman, 1988) and consideration of exchange equilibria between olivine and orthopyroxene require substantial positive deviations from ideality for ferromagnesian olivine solutions. Their model is taken as a starting point for calibration of multicomponent olivine models, and their Fe-Mg interaction parameters are adopted directly (Table 6). The mixing parameters recommended by Sack and Ghiorso (1989) may, however, ultimately require minor revisions. Although their model assumes zero ordering energy, site occupancy data indicate a weak affinity for Fe in the M1 site that increases with temperature (Aikawa et al., 1985; Motoyama and Matsumoto, 1989; Ottonello et al., 1990). This argues for a small enthalpy and entropy of ordering. Sack and Ghiorso (1989) also assume that the site-specific regular-solution parameters are equivalent ( $W_{FeMg}^{M1} = W_{FeMg}^{M2}$ ), but accumulated data suggest that degree of ordering correlates with fayalite content (Motoyama and Matsumoto, 1989), which suggests that there are small differences between  $W_{FeMg}^{M1}$  and  $W_{FeMg}^{M2}$ .

### Nickel magnesium iron olivines

Calibration of Ni-bearing olivines begins with consideration of octahedral site preferences. Before evaluating the available cation ordering data, it is necessary to consider the effect of thermal history on the ordering state of

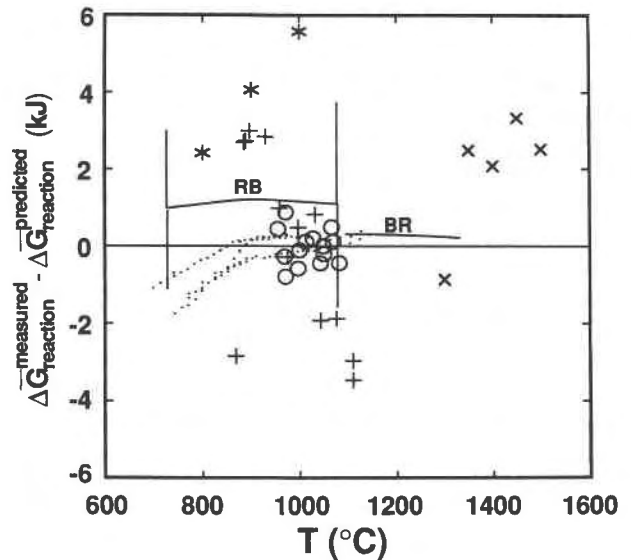


Fig. 1. Calculated minus experimentally determined Gibbs energy of reaction  $2Ni + SiO_2 + O_2 = Ni_2SiO_4$ . Symbols: x = Campbell and Roeder (1968); stars = Taylor and Schmalzried (1964); pluses = Ottonello and Morlotti (1987); open circles = Levitskii et al. (1975); dots = O'Neill (1987); line marked BR = Boström and Rosén (1988); line marked RB is comparison to experimentally determined Gibbs energy of reaction  $2NiO + SiO_2 = Ni_2SiO_4$ , Rog and Borchardt (1984) with 1 s.d. error bars. For internal consistency, the chemical potential of Ni-NiO reference electrodes for emf studies of Levitskii et al., O'Neill, Boström and Rosén, and Ottonello and Morlotti are calculated using Hemingway (1990).

olivines, as the kinetics of intracrystalline ordering are known to be strongly temperature dependent (e.g., Aikawa et al., 1985; Anovitz et al., 1988). Equilibrium ordering states are not quenchable from high temperature, and achieving equilibrium at low temperature may require extended heat treatment.

The study of Aikawa et al. (1985), in which samples were quenched in 10 ms, demonstrates that equilibrium ordering states of olivine cannot be quenched from temperatures above 700–900 °C. Cation distributions of samples quenched from temperatures greater than 800 °C are therefore assumed to be more ordered than the equilibrium state at the temperature of annealing. Although there are no data to constrain the time required for olivines to achieve equilibrium ordering at low temperatures, orthopyroxenes heated for 6 weeks at temperatures < 600 °C do not attain homogeneous equilibrium (Anovitz et al., 1988). As the high-temperature intracrystalline kinetics of orthopyroxene are similar to those of olivine (Aikawa et al., 1985; Anovitz et al., 1988), it is assumed that olivines annealed at temperatures 600 °C and lower for times less than several weeks did not reach equilibrium.

With these limitations in mind, ordering along the  $Ni_2SiO_4$ - $Mg_2SiO_4$  binary may be examined. Here,  $X_{Fe}^{O_2} = 0$ ,  $r = -1$ , and  $s = 0$ . Substituting these values into the

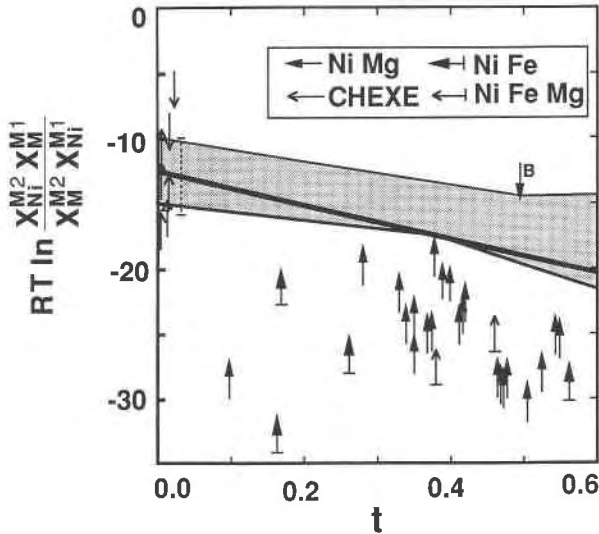


Fig. 2. Intracrystalline cation distributions for Ni-bearing olivines.  $RT \ln(X_{Ni}^{M2} X_{Mg}^{M1} / X_{Mg}^{M2} X_{Ni}^{M1})$  vs. ordering variable  $t (= X_{Ni}^{M1} - X_{Ni}^{M2})$ ,  $M = Mg$  for Ni-Mg and CHEXE samples,  $M = Fe$  for nickel iron and nickel magnesium iron olivines. All samples were quenched from 800 °C or hotter except as noted below. CHEXE samples include nearly completely ordered natural olivines (Smyth and Tafto, 1982) and disordered synthetic olivines (McCormick et al., 1987), each annealed at 300 °C (6–9 d) and 600 °C (2 d), which are assumed to be more and less ordered, respectively, than the equilibrium state for the temperature of treatment. Synthetic nickel magnesium olivine (Bish, 1981) (marked B), synthesized at 500 °C and 2.1 kbar for 4 weeks, is assumed to be less ordered than equilibrium state. Error bar is representative 1 s.d. for CHEXE data. Shaded area is region of fits permitted by data; straight line is preferred fit to data (see text).

expression for equilibrium ordering between Ni and Mg (Appendix 1, Eq. A2) gives

$$0 = \left( \frac{\partial \bar{G}}{\partial t} \right)_q = \frac{1}{2} \left[ RT \ln \left( \frac{X_{Ni}^{M1} X_{Mg}^{M2}}{X_{Mg}^{M1} X_{Ni}^{M2}} \right) + \Delta \bar{H}_{EX}^{MgNi} + t(\Delta \bar{H}_X^{MgNi} - W_{MgNi}^{M1} - W_{MgNi}^{M2}) + q(W_{MgNi}^{M2} - W_{MgNi}^{M1}) \right]. \quad (19a)$$

If we assume that  $W_{MgNi}^{M1} = W_{MgNi}^{M2} = W_{MgNi}^{OI}$ , which is equivalent to assuming that there is no compositional dependence on ordering energy (see discussion below), the expression for the equilibrium ordering state reduces to

$$RT \ln \left( \frac{X_{Ni}^{M2} X_{Mg}^{M1}}{X_{Mg}^{M2} X_{Ni}^{M1}} \right) = \Delta \bar{H}_{EX}^{MgNi} + t(\Delta \bar{H}_X^{MgNi} - 2W_{MgNi}^{OI}). \quad (19b)$$

Values for  $\Delta \bar{H}_{EX}^{MgNi}$  and  $(\Delta \bar{H}_X^{MgNi} - 2W_{MgNi}^{OI})$  can therefore be extracted from the slope and intercept of a plot of

$$RT \ln \left( \frac{X_{Ni}^{M2} X_{Mg}^{M1}}{X_{Mg}^{M2} X_{Ni}^{M1}} \right)$$

vs.  $t$ .

Ordering in synthetic and natural nickel magnesium olivines has been determined by X-ray refinement (Rajamani et al., 1975; Bish, 1981; Boström, 1987; Ottonello et al., 1989) and polarized optical absorption spectroscopy (Hu et al., 1990; Fig. 2). All determinations of synthetic olivines indicate partial ordering of Ni on the M1 site. Channeling enhanced X-ray emission spectroscopy (CHEXE) examination of trace quantities of Ni in heat-treated San Carlos olivine (Smyth and Tafto, 1982) and synthetic magnesium iron olivines doped with minor concentrations of Ni (McCormick et al., 1987) also indicate Ni enrichment on M1, though ordering is less pronounced than in more Ni-rich crystals.

The data in Figure 2 are consistent with ordering energies greater than 10 kJ, but given the wide brackets provided by observations of Fe-free olivines and the large uncertainties associated with CHEXE determinations, a range in values of  $\Delta \bar{H}_{EX}^{MgNi}$  and  $(\Delta \bar{H}_X^{MgNi} - 2W_{MgNi}^{OI})$  potentially satisfies the site occupancy constraints (Fig. 2). Specific values for  $\Delta \bar{H}_{EX}^{MgNi}$  and  $(\Delta \bar{H}_X^{MgNi} - 2W_{MgNi}^{OI})$  consistent with the range outlined in Figure 2 may be selected only from additional constraints imposed by measured activity-composition relations and exchange equilibria discussed below.

The energy of ordering along the Ni-Fe binary may be examined by imposing the condition of homogeneous equilibrium

$$\left( \frac{\partial \bar{G}}{\partial s} \right)_{q,r,t} + \left( \frac{\partial \bar{G}}{\partial t} \right)_{q,r,s} = 0. \quad (20)$$

Substituting expressions A1 and A2 (Appendix 1) and recognizing that  $q = -r$  and  $s = t$  in the Mg-free case gives

$$0 = \left( \frac{\partial \bar{G}}{\partial s} \right)_{q,r,t} + \left( \frac{\partial \bar{G}}{\partial t} \right)_{q,r,s} = \frac{1}{2} \left[ RT \ln \left( \frac{X_{Ni}^{M2} X_{Fe}^{M1}}{X_{Fe}^{M2} X_{Ni}^{M1}} \right) + \Delta \bar{H}_{EX}^{FeNi} + t(\Delta \bar{H}_X^{FeNi} - W_{FeNi}^{M1} - W_{FeNi}^{M2}) + q(W_{FeNi}^{M2} - W_{FeNi}^{M1}) \right]. \quad (21a)$$

By again equating the site-specific interaction terms,  $W_{FeNi}^{M1} = W_{FeNi}^{M2} = W_{FeNi}^{OI}$ , Equation 21a reduces to

$$RT \ln \left( \frac{X_{Ni}^{M1} X_{Fe}^{M2}}{X_{Fe}^{M1} X_{Ni}^{M2}} \right) = \Delta \bar{H}_{EX}^{FeNi} + t(\Delta \bar{H}_X^{FeNi} - 2W_{FeNi}^{OI}) \quad (21b)$$

and  $\Delta \bar{H}_{EX}^{FeNi}$  and  $(\Delta \bar{H}_X^{FeNi} - 2W_{FeNi}^{OI})$  may again be extracted from a plot of the distribution coefficients vs. the ordering variable  $t$  (Fig. 2). Annersten et al. (1982; data corrected in Annersten and Philippidis, 1984) reported Mössbauer spectra from synthetic iron nickel olivines heat treated at

1000 °C and quenched in air (Fig. 2). The site occupancies of these olivines are similar to those of nickel magnesium olivines with similar thermal histories, and it is reasonable to assume that the energy of ordering between Ni and Fe is equivalent to that between Ni and Mg.

Site occupancy measurements of iron nickel magnesium olivines containing ~50 mol% Mg give similar Fe-Ni distributions to Mg-free samples (Nord et al., 1982; Fig. 2). The similarity between the site distributions for iron nickel olivines and iron nickel magnesium olivines supports the assumption that the ordering energies of Fe-Ni and Mg-Ni interactions are similar. This can be demonstrated by summing Equations A1 and A2 and setting  $\Delta\bar{H}_{EX}^{FeMg}$  and  $(\Delta\bar{H}_X^{FeMg} - W_{FeMg}^{M1} - W_{FeMg}^{M2})$  equal to 0 (Table 6). The resulting expression is

$$\begin{aligned}
 RT \ln \left( \frac{X_{Ni}^{M1} X_{Fe}^{M2}}{X_{Fe}^{M1} X_{Ni}^{M2}} \right) &= \Delta\bar{H}_{EX}^{FeNi} + \frac{(q+r)}{2} (\Delta\bar{H}_{EX}^{FeNi} - \Delta\bar{H}_{EX}^{MgNi}) \\
 &+ \frac{(t+s)}{2} (\Delta\bar{H}_X^{FeNi} - 2W_{FeNi}^{OI}) \\
 &+ \frac{(t-s)}{2} (\Delta\bar{H}_X^{MgNi} - 2W_{MgNi}^{OI}). \quad (22)
 \end{aligned}$$

Comparison of Equation 22 with Equation 21b shows that Ni-Fe ordering is effectively independent of Mg content only if  $\Delta\bar{H}_{EX}^{FeNi}$  and  $\Delta\bar{H}_{EX}^{MgNi}$  are approximately equal and if the  $(\Delta\bar{H}_X - 2W^{OI})$  terms are similar.

Activity-composition relations of nickel magnesium olivines have been determined directly by gas mixing experiments (Campbell and Roeder, 1968) and by emf studies (Ottonello and Morlotti, 1987; Boström and Rosén, 1988). The data of Boström and Rosén (1988) are given the most weight because their measurements for pure  $Ni_2SiO_4$  show greater internal consistency than do the others (Fig. 1). The activity-composition measurements of Ottonello and Morlotti (1987) are in serious disagreement with all other available data and are therefore discounted.

Negative deviations from ideality measured at low and intermediate mole fractions of  $Ni_2SiO_4$  ( $0 \leq X_{Ni_2SiO_4} \leq 0.51$ ) (Figs. 3a–3c) require that contributions to the energy of mixing from ordering [as represented by the  $\Delta\bar{H}_{EX}^{MgNi}$  and  $(\Delta\bar{H}_X^{MgNi} - 2W_{MgNi}^{OI})$  terms] be greater than that from positive regular-solution-like interactions [represented by  $(\Delta\bar{H}_X^{MgNi} + 2W_{MgNi}^{OI})$  over that range of composition and temperature. Small values of  $(\Delta\bar{H}_X^{MgNi} + 2W_{MgNi}^{OI})$  yield the best fits to these data, as measured by the standard deviation. Among the ordering variables, the standard deviation is minimized by using the most negative value for  $(\Delta\bar{H}_X^{MgNi} - 2W_{MgNi}^{OI})$  permitted by the site occupancy constraints for a given  $\Delta\bar{H}_{EX}^{MgNi}$  (Fig. 2), but it is not strongly sensitive to the specific  $\Delta\bar{H}_{EX}^{MgNi}$  used.

The final constraints available to calibrate nickel magnesium olivine solution properties are Ni-Mg exchange

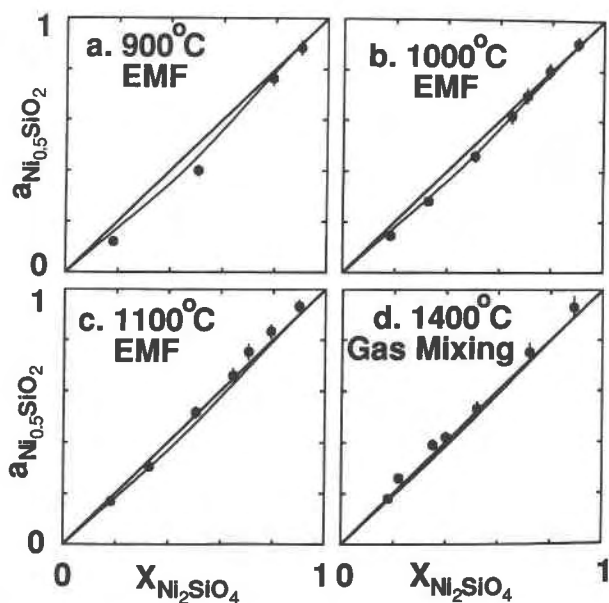


Fig. 3. Direct activity measurements. Circles are experimental data with 2 s.d. error bars; solid lines are calculated activities. (a)–(c) EMF determinations at 900, 1000, and 1100 °C (Boström and Rosén, 1988). (d) Gas mixing experiments at 1400 °C (Campbell and Roeder, 1968).

experiments between olivine and oxide at 5 kbar and 1300 °C and 1 bar and 923 °C (Seifert and O'Neill, 1987). Calibration of olivine mixing parameters from these data requires determination of the mixing properties of NiO-MgO oxides. The experimental results for this solution are contradictory, but most studies indicate either nearly ideal behavior (e.g., Hahn and Muan, 1961; Paulsson, 1982) or negative deviations from ideality (e.g., Evans and Muan, 1971; Davies and Navrotsky, 1981). Davies and Navrotsky (1981) attributed negative departures from ideality to convergent ordering of Ni and Mg atoms in the rocksalt structure, which is consistent with HRTEM observations of ordered domains (Davies et al., 1980). Given the lack of agreement between the various determinations, it was deemed best to determine the mixing properties of the oxides along with the remaining olivine mixing parameters by consideration of the experimental exchange data. The sources for the adopted standard state properties of the oxides are listed in Appendix 2.

Seifert and O'Neill (1987) propose that oxide-olivine exchange equilibria may be fitted by treating magnesium nickel oxides as nearly ideal, but their analysis neglects the effect of ordering in olivines. If we assume ideal mixing in the oxide phase and apply values of  $\Delta\bar{H}_{EX}^{MgNi}$  and  $(\Delta\bar{H}_X^{MgNi} - 2W_{MgNi}^{OI})$  consistent with the constraints developed above, then it should be possible to fit the exchange data by adjusting  $(\Delta\bar{H}_X^{MgNi} + 2W_{MgNi}^{OI})$ , but any values for this grouped variable yield poor fits to the 5 kbar exchange data (Fig. 4a). This result is not sensitive to the specific values of  $\Delta\bar{H}_{EX}^{MgNi}$  and  $(\Delta\bar{H}_X^{MgNi} - 2W_{MgNi}^{OI})$  used. Adopting small negative deviations from ideality for the



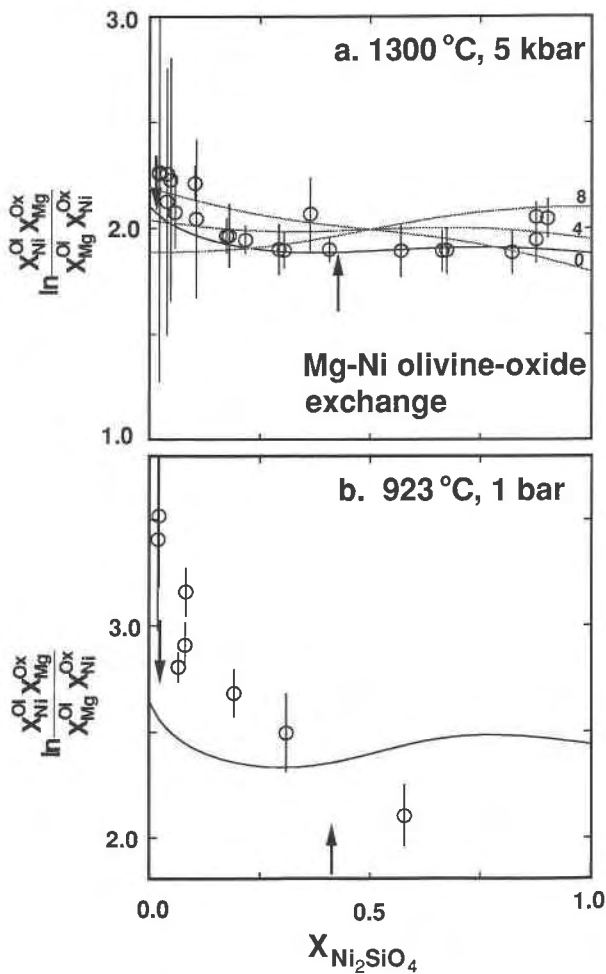


Fig. 4. Olivine-oxide exchange equilibria (Seifert and O'Neill, 1987). Circles are unreversed synthesis experiments with 1 s.d. error bars; arrows are reversal half brackets. (a) 1300 °C and 5 kbar. Dashed lines are attempted fits to data with oxides assumed ideal and  $(\Delta\bar{H}_X^{\text{MgNi}} + 2W_{\text{MgNi}}^{\text{Ox}})$  equal to 0, 4, and 8 kJ. Solid line is preferred fit to data. (b) 923 °C and 1 bar. Solid line is preferred fit to data. Experiments at this temperature did not reach equilibrium (see text).

oxides ( $W_{\text{MgNi}}^{\text{Ox}} = -1.8$  kJ), however, permits markedly improved matches to these data. Because this interaction term probably proxies for an ordering energy, it is likely to be temperature dependent. Reasonable fits to the activity-composition and exchange data are achieved by setting  $\Delta\bar{H}_{\text{EX}}^{\text{MgNi}}$ ,  $(\Delta\bar{H}_X^{\text{MgNi}} - 2W_{\text{MgNi}}^{\text{Ox}})$ , and  $(\Delta\bar{H}_X^{\text{MgNi}} + 2W_{\text{MgNi}}^{\text{Ox}})$  equal to  $-12.5 \pm 2.5$ ,  $-13.0 \pm 3.0$ , and  $2.2 \pm 0.5$  kJ, respectively (Figs. 3, 4). Better fits to the exchange data for Ni-rich compositions and poorer fits for Ni-poor compositions are given by more negative values of  $\Delta\bar{H}_{\text{EX}}^{\text{MgNi}}$ , and the opposite is true for less negative values. However, the overall quality of the fit is not strongly sensitive to the ordering energy within the limits developed from site occupancy and activity measurements. Better fits to the exchange data are possible with larger values

of  $(\Delta\bar{H}_X^{\text{MgNi}} + 2W_{\text{MgNi}}^{\text{Ox}})$  but only at the expense of poorer fits to the activity measurements.

The mixing parameters chosen from 1300 °C and applied to the same exchange equilibria at 1 bar and 923 °C (Seifert and O'Neill, 1987; Fig. 4b) give a fit consistent with the reversal experiments but fail to fit the unreversed synthesis experiments. This is a satisfactory result because, as recognized by Seifert and O'Neill (1987), the durations of the 1 bar experiments were insufficient by 2 orders of magnitude to achieve equilibrium. The negative excess Gibbs energy of the oxides is probably not appropriately modeled by the  $W_{\text{MgNi}}^{\text{Ox}}$  value extracted from the high-temperature data, but the reversal experiments alone are not sufficient to determine the temperature dependence of this parameter. The reversal data at 923 °C would be better fitted by increasing the magnitude of  $W_{\text{MgNi}}^{\text{Ox}}$ , which is consistent with the supposition that nonideality is the result of ordering.

The positive deviations from ideality at high Ni contents indicated by activity measurements (Fig. 3c) could be accommodated by the solution model only if  $W_{\text{MgNi}}^{\text{M2}}$  were substantially greater than  $W_{\text{MgNi}}^{\text{M1}}$ . Possible inequality between these parameters has a physical basis, as the geometrically distinct octahedral sites of olivines must differ energetically, but intuition suggests that larger interaction energies would be associated with the smaller M1 site. Setting  $W_{\text{MgNi}}^{\text{M2}} > W_{\text{MgNi}}^{\text{M1}}$  would diminish the quality of the proposed fit to the olivine-oxide exchange reaction, causing a sharp drop in predicted distribution coefficient at high Ni contents that is not seen in the data (Fig. 4); if anything, the opposite is suggested. Inequality between the site-specific interaction parameters would also indicate a linear compositional dependence on ordering that is not seen in the site occupancy data as a whole or among olivines with identical thermal histories (Boström, 1987). In the absence of more compelling evidence for unequal interaction parameters, the assumption that  $W_{\text{MgNi}}^{\text{M2}} = W_{\text{MgNi}}^{\text{M1}}$  is retained.

As there are no exchange equilibria or direct activity measurements available to constrain  $(\Delta\bar{H}_X^{\text{FeNi}} + 2W_{\text{FeNi}}^{\text{Ox}})$ , it is assumed to be equal to  $(\Delta\bar{H}_X^{\text{MgNi}} + 2W_{\text{MgNi}}^{\text{Ox}})$ . The validity of this assumption is partially confirmed by examination of olivine-alloy equilibria (see below), but for Mg-rich olivines the potential error introduced by this assumption will be small in any event. Values for the derived set of solution parameters for nickel magnesium iron olivines are given in Table 6.

As is evident from the foregoing discussion, considerable uncertainty about the specific solution parameters for nickel magnesium iron olivines remain. The solution parameters chosen are consistent with the available data, but improved resolution of these parameters is desirable. In particular, tighter restrictions on the ordering energy of nickel magnesium olivines are required to obtain a more certain set of solution parameters.

**Volume of mixing.** Olivine solid solutions generally show positive deviations from Vegard's law (Matsui and Syono, 1968), much of which may be attributed to or-

dering. Volume dependent mixing parameters may be derived from pressure derivatives of enthalpy of mixing parameters, e.g.,

$$\Delta \bar{V}_{\text{EX}}^{\text{MgNi}} = \left( \frac{\partial \Delta \bar{H}_{\text{EX}}^{\text{MgNi}}}{\partial P} \right)_T \quad (23a)$$

$$W_{\text{MgNi}}^{\text{VM1}} = \left( \frac{\partial W_{\text{MgNi}}^{\text{M1}}}{\partial P} \right)_T \quad (23b)$$

Assuming that the site-specific volume interaction terms are equal,  $W_{\text{MgNi}}^{\text{VM1}} = W_{\text{MgNi}}^{\text{VM2}} = W_{\text{MgNi}}^{\text{V}}$ , and that volume of disorder is a linear function of ordering state, the excess volume owing to ordering for magnesium nickel olivines is

$$\Delta \bar{V}_{\text{MgNi}}^{\text{DIS}} = \frac{1}{2} \Delta \bar{V}_{\text{EX}}^{\text{MgNi}} (t_a - t_b) \quad (24)$$

(Sack and Ghiorso, 1989), where  $t_a$  and  $t_b$  refer to two different ordering states, and the excess volume of mixing is

$$\Delta \bar{V}_{\text{MgNi}}^{\text{XS}} = \frac{1}{2} \Delta \bar{V}_{\text{EX}}^{\text{MgNi}} t + \frac{1}{4} (\Delta \bar{V}_{\text{X}}^{\text{MgNi}} + 2W_{\text{MgNi}}^{\text{V}}) \quad (25)$$

(Sack and Ghiorso, 1989). Equivalent expressions may be developed for iron nickel olivines.

Unit-cell parameters of several magnesium nickel olivines of nearly identical composition but different ordering states (Fig. 5a) are reported by Boström (1987) and Ottonello et al. (1989). The olivines were synthesized under identical conditions (Boström, 1987), and corrections for compositional differences between crystals are much smaller than analytical uncertainty for cell volumes. Linear regression of these data using Equation 24 gives  $\Delta \bar{V}_{\text{EX}}^{\text{MgNi}} = 0.035 \pm 0.012$  J/bar.

The compositional dependence of excess volume for magnesium nickel olivines may be estimated from measured lattice parameters across the binary (Matsui and Syono, 1968; Rajamani et al., 1975; Bish, 1981; Boström, 1987; Ottonello et al., 1989). Setting  $(\Delta \bar{V}_{\text{X}}^{\text{MgNi}} + 2W_{\text{MgNi}}^{\text{V}})$  equal to  $-0.01 \pm 0.01$  J/bar gives good approximations to the measured excess volumes at reasonable blocking temperatures (Fig. 5b).

As there are no data pertaining directly to the volume of ordering for iron nickel olivines,  $\Delta \bar{V}_{\text{EX}}^{\text{FeNi}}$  is presumed to be the same as  $\Delta \bar{V}_{\text{EX}}^{\text{MgNi}}$ . The few lattice parameter measurements available for iron nickel olivines (Annersten et al., 1982), though relatively imprecise, are consistent with equating  $\Delta \bar{V}_{\text{EX}}^{\text{FeNi}}$  with  $\Delta \bar{V}_{\text{EX}}^{\text{MgNi}}$  and  $(\Delta \bar{V}_{\text{X}}^{\text{FeNi}} + 2W_{\text{FeNi}}^{\text{V}})$  with  $(\Delta \bar{V}_{\text{X}}^{\text{MgNi}} + 2W_{\text{MgNi}}^{\text{V}})$  (Fig. 5b).

### Calcium magnesium iron olivines

The mixing properties of Ca-bearing olivines may be calibrated from consideration of experimentally determined miscibility gaps (Mukhopadhyay and Lindsley, 1983; Davidson and Mukhopadhyay, 1984; Adams and Bishop, 1985) and from consideration of olivine-pyroxene exchange experiments (e.g., Adams and Bishop, 1986;

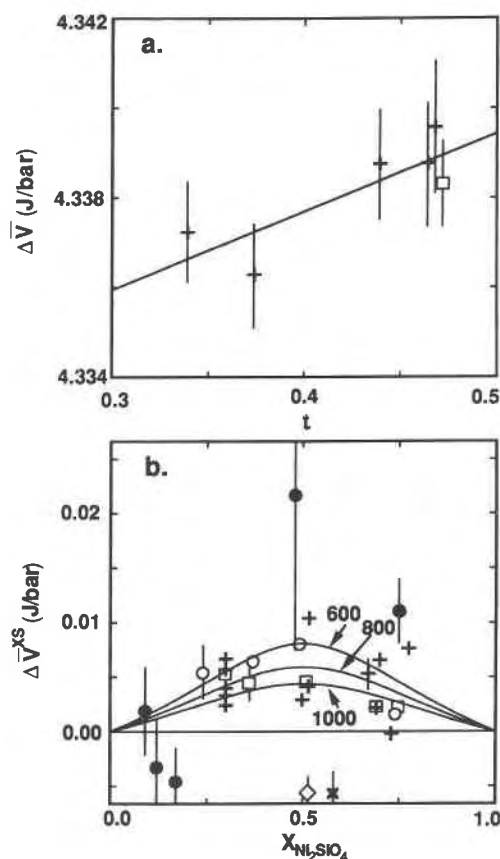


Fig. 5. (a) Molar volume of olivine with  $X_{\text{Ni}_2\text{SiO}_4} = 0.3$  and variable degrees of order. Error bars are 2 s.d. Straight line is linear regression of data, giving  $\Delta \bar{V}_{\text{EX}}^{\text{MgNi}} = 0.035 \pm 0.012$  J/bar mol. (b) Excess volumes of magnesium nickel and iron nickel olivines. Representative error bars are 1 s.d. Solid lines = predicted excess volumes at 600, 800, and 1000 °C with  $(\bar{V}_{\text{X}}^{\text{MgNi}} + 2W_{\text{MgNi}}^{\text{V}}) = -0.01 \pm 0.01$  J/bar. Data sources for a and b: open circles = Matsui and Syono (1968); open squares = Boström (1987); crosses = Ottonello et al. (1989); diamond = Rajamani et al. (1975); x = Bish (1981). Filled circles = iron nickel olivines, Annersten et al. (1982).

Davidson and Lindsley, 1989), provided a consistent model for quadrilateral pyroxenes is employed. Because the mixing properties of pyroxenes are beyond the scope of this paper, the mixing properties of Ca-bearing olivines are calibrated here solely from miscibility constraints. The parameters so derived may later require adjustment subject to consideration of the constraints imposed by olivine-pyroxene equilibria.

For calcian olivines, only three mixing parameters must be calibrated:  $W_{\text{CaMg}}^{\text{M2}}$ ,  $W_{\text{CaFe}}^{\text{M2}}$ , and  $\bar{F}^0$ . Along the Fe-free binary,  $r = -1$ ,  $s = 0$ , and the quadrilateral model reduces to a simple symmetric regular solution dependent on  $W_{\text{CaMg}}^{\text{M2}}$ . The reversed experiments of Adams and Bishop (1985) indicate a slightly asymmetric solvus along the monticellite-forsterite join, particularly at 5 kbar (Fig. 6), but asymmetry cannot be accommodated by the adopted formulation. Instead,  $W_{\text{CaMg}}^{\text{M2}}$  is chosen to best approxi-

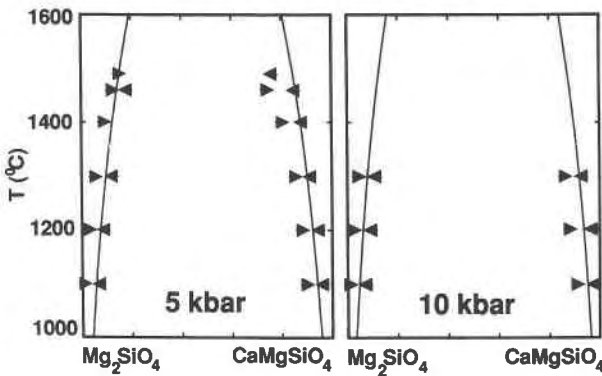


Fig. 6. Miscibility gap in CaMgSiO<sub>4</sub>-Mg<sub>2</sub>SiO<sub>4</sub> olivines at 5 and 10 kbar. Data (arrows) from Adams and Bishop (1986). Solid lines are calculated solvi.

mate the the Ca-poor limb of the solvus. Setting  $W_{CaMg}^{M2}$  equal to  $34.5 \pm 1.0$  kJ and  $(\partial W_{CaMg}^{M2} / \partial P)_T = 0.35$  J/bar produces reasonable fits to both limbs of the experimentally determined solvus at 10 kbar and the Ca-poor limb at 5 kbar (Fig. 6). Inability to fit the Ca-rich limb of the solvus at high temperature has only a negligible effect on calculated chemical potentials of calcian components of typical ferromagnesian olivines.

The limits of miscibility of calcium iron olivines are determined from reversed two-phase experiments at 1 bar and 1 kbar (Mukhopadhyay and Lindsley, 1983) that delineate a symmetric solvus with a critical point at about 1040 °C. The value for  $W_{CaFe}^{M2}$  ( $21.9 \pm 0.1$ ) derived by Mukhopadhyay and Lindsley (1983) from these data is adopted here.

The remaining uncalibrated term,  $\bar{F}^0$ , is evaluated by consideration of the length and orientation of tie lines across the solvus for calcium magnesium iron olivines determined by Davidson and Mukhopadhyay (1984). A reasonable match between predicted and experimentally determined tie lines is achieved with  $\bar{F}^0 = 9.5 \pm 1.0$  kJ (Fig. 7). The preferred set of mixing parameters for calcium magnesium iron olivines is summarized in Table 7.

**RESULTS AND DISCUSSION**

**Nickel magnesium iron olivines**

The derived model predicts negative deviations from ideality across the magnesium nickel and iron nickel olivine binaries (e.g., Fig. 3), although these deviations are small at high temperature. While this prediction is consistent with the frequently cited experimental results of Campbell and Roeder (1968) (Fig. 3d), it does not justify the common assumption (e.g., Campbell et al., 1979; Doyle and Naldrett, 1987; Fleet and MacRae, 1988;

TABLE 7. Solution properties of calcium magnesium iron olivines

$W_{CaMg}^{M2}$	$34.5 \pm 2.0$ kJ	$W_{CaFe}^{M2}$	$21.9 \pm 0.1$ kJ*
$\bar{F}^0$	$9.5 \pm 1.0$ kJ	$(\partial W_{CaMg}^{M2} / \partial P)_T$	0.35 J/bar

Note: See Table 6 for Fe-Mg interaction parameters.

\* Mukhopadhyay and Lindsley (1983).

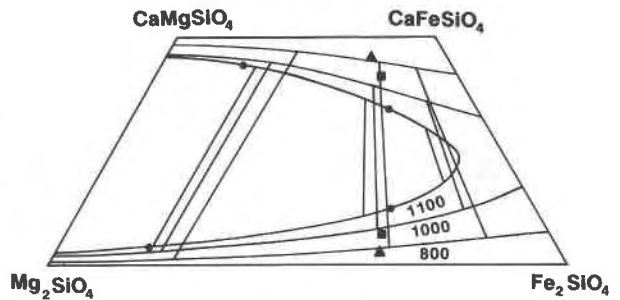


Fig. 7. Miscibility gap in calcium magnesium iron olivines. Coexisting pairs: triangles = 800 °C, 1 kbar; squares = 1000 °C, 1 bar; circles = 1100 °C, 1 bar (Davidson and Mukhopadhyay, 1984). Predicted solvi and tie lines are at 800 °C, 1 kbar; 1000 °C, 1 bar; and 1100 °C, 1 bar.

Kinzler et al., 1990) that mixing of Ni<sub>2</sub>SiO<sub>4</sub> in ferromagnesian olivines is ideal. The ideal approximation is inadequate because the effect of ordering on the chemical potential of Ni<sub>2</sub>SiO<sub>4</sub> and the cooperative effect of excess energies from Mg-Fe interactions increase departures from ideal behavior relative to that observed on the Ni-Mg and Ni-Fe binaries. These phenomena are illustrated in Figure 8, where calculated single-site activity coefficients,  $\gamma$ ,

$$\gamma_{NiSiO_2} = \frac{(a_{Ni_2SiO_4})^{1/2}}{X_{Ni_2SiO_4}} \tag{26}$$

are plotted against  $X_{Fe}^{OI} / (X_{Fe}^{OI} + X_{Mg}^{OI})$  at constant Ni concentration,  $X_{Ni_2SiO_4}^{OI} = 0.005$  [ $X_{Ni_2SiO_4}^{OI} = 0.005$  equals 4150 ppm Ni in otherwise pure forsterite ( $X_{Mg_2SiO_4}^{OI} = 0.995$ ) and 2880 ppm Ni in otherwise pure fayalite ( $X_{Fe_2SiO_4}^{OI} = 0.995$ )], over a range of temperatures. Activity coefficients in the binary systems are temperature dependent and range from 0.98 at 1400 °C to just over 0.92 at 900 °C. Negative deviations from ideality become more pronounced moving from the bounding binaries into the ternary system. The value of  $\gamma_{NiSiO_2}$  is 0.86 at 1200 °C for compositions typical of primitive basalt (Fo<sub>85</sub>) and correspondingly lower for more fayalitic olivines. Positive volumes of ordering in olivine solutions cause a reduction of ordering at elevated pressures, but the effects on the mixing properties of trace components are small. Predicted activity coefficients in Fo<sub>90</sub> at 1300 °C increase by less than 2% between 1 bar and 50 kbar.

The approach taken here differs from that of several other recent thermodynamic treatments of Ni solution in olivine (Seifert and O'Neill, 1987; Colson et al., 1988; Seifert et al., 1988; Fleet, 1989) in that the present study begins with the standard state properties of the end-members and considers both intercrystalline and intracrystalline equilibria.

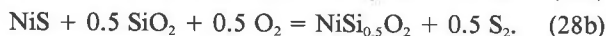
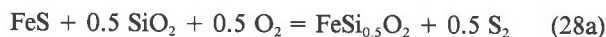
Seifert and O'Neill (1987) fitted nickel magnesium olivines to a regular solution model using exchange equilibria between olivine and oxides at 1300 °C. They predicted slight positive departures from ideality ( $W_{MgNi}^{OI} = 0.351$  kJ). Seifert et al. (1988) extended this analysis to

nickel magnesium iron olivines by treating Mg-Fe interactions with a symmetric regular-solution interaction parameter ( $W_{\text{MgFe}}^{\text{OI}} = 6.28 \text{ kJ}$ ) from Kawasaki and Matsui (1983), giving

$$RT \ln \gamma_{\text{NiSi}_{0.5}\text{O}_2}^{\text{OI}} = W_{\text{MgNi}}^{\text{OI}} (X_{\text{MgSi}_{0.5}\text{O}_2}^{\text{OI}} + X_{\text{FeSi}_{0.5}\text{O}_2}^{\text{OI}})^2 - W_{\text{MgFe}}^{\text{OI}} (X_{\text{MgSi}_{0.5}\text{O}_2}^{\text{OI}} X_{\text{FeSi}_{0.5}\text{O}_2}^{\text{OI}}). \quad (27)$$

Their model predicts nearly ideal behavior for binary nickel magnesium olivines and small negative deviations from ideality for ternary olivines with intermediate Fe/(Fe + Mg) contents (Fig. 8). Application of this model to experimental equilibria between olivine and FeNi alloy (Seifert et al., 1988) results in systematic discrepancies that result in part from the values used for standard state properties, but Seifert et al. (1988) suggest that improvements of their formulation could also be achieved by treating the effect of ordering or by using a larger Fe-Mg interaction parameter. These are the primary distinctions between their analysis and the present one.

Fleet (1989) derived activity coefficients for  $\text{NiSi}_{0.5}\text{O}_2$  from experiments with nickel magnesium iron olivines coexisting with (Fe,Ni)S liquids over a range of compositions at known  $f_{\text{S}_2}$  and  $f_{\text{O}_2}$  and fixed temperature by considering the reactions



He did this by (a) calculating activities of FeS from Equation 28a, using activity coefficients for  $\text{FeSi}_{0.5}\text{O}_2$  in olivine from the equation of Williams (1972); (b) calculating NiS activities by graphically integrating the Gibbs-Duhem equation across the FeS-NiS pseudobinary; and then (c) using the calculated NiS activities to calculate  $\text{NiSi}_{0.5}\text{O}_2$  activities from Equation 28c. The results predict strong positive deviations from ideality and marked deviations from Henry's Law for compositions between <0.1 and 1.2 mol%  $\text{Ni}_2\text{SiO}_4$  (Fig. 8), but they are not likely to be correct for the following reasons: (1) Activities of  $\text{FeSi}_{0.5}\text{O}_2$ , calculated from the regression equation of Williams (1972), are probably underestimated (Sack and Ghiorso, 1989). (2) Derivation of activities in methods a and c require the assumption that  $a_{\text{SiO}_2}$  was constant in unbuffered experiments, although this may not have been the case. (3) The Gibbs-Duhem integration was performed across a pseudobinary over which the chemical potentials of other components were not held constant, and it is therefore invalid. (4) The sum of propagated errors from calculations a through c, both analytical and those inherited from 1-3, are undoubtedly very large.

Colson et al. (1989) calculate Henry's Law activity coefficients for the species  $\text{MgNiSiO}_4$  in olivine by linear regression of olivine-silicate liquid distributions, assuming ideal mixing in the liquid and between Fe and Mg in olivine. (The order in which divalent cations are written does not connote specific site occupancy in Colson et al., 1989.) Although the activity of the species  $\text{MgNiSiO}_4$  is not directly comparable to  $(a_{\text{Ni}_2\text{SiO}_4})^{0.5}$ , its predicted de-

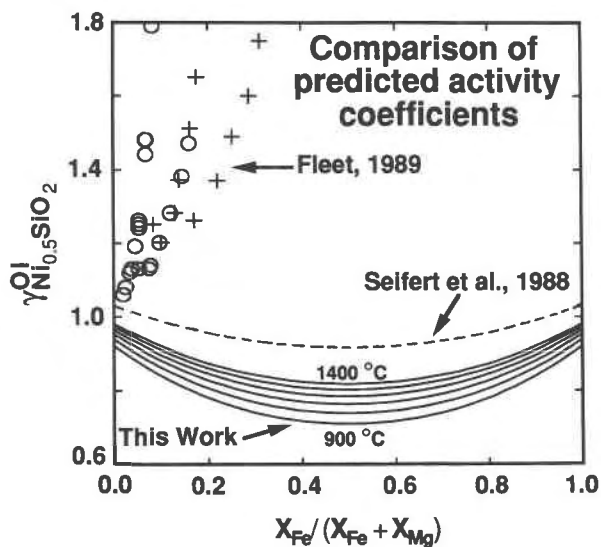


Fig. 8. Predicted single-site activity coefficients for nickel olivine. Circles = Fleet (1989) at 1385 and 1395 °C; crosses = Fleet (1989) at 1300 and 1307 °C; dashed line = calculated from solution model of Seifert et al. (1988) (1300 °C); solid lines = calculated from present model at 900, 1000, 1100, 1200, 1300, and 1400 °C.  $\text{Ni}_2\text{SiO}_4$  concentration for samples from Fleet (1989) range from 0.0006 to 0.0126 mol%; other calculations are for  $X_{\text{Ni}_2\text{SiO}_4} = 0.005$ .

partures from ideality for solution of Ni in olivine are qualitatively similar to those calculated here for compositions between  $\text{Fo}_{100}$  and  $\text{Fo}_{50}$ , within the uncertainty of their regression. Colson et al. (1989) interpret departures from ideal solution of Ni and other trace cations (Tr) in olivine as evidence for differences between Tr-Fe and Tr-Mg short-range interactions because the residuals of their regression correlate with olivine forsterite content. This correlation, however, is probably caused in part by non-ideal Fe-Mg interactions, which they neglect.

### Calcium magnesium iron olivines

The formulation adopted for Ca-bearing olivines is very similar to that developed by Davidson and Mukhopadhyay (1984), and the calibrated mixing parameters are similar to the values recommended by Davidson and Mukhopadhyay (1984) and Davidson and Lindsley (1989). The chief difference between previous models and the present one is the larger  $W_{\text{MgFe}}^{\text{OI}}$  interaction energy adopted here. The primary shortcoming of both the present formulation and that of Davidson and Mukhopadhyay (1984) is that neither accommodates the asymmetry of the experimentally determined monticellite-forsterite solvus (Adams and Bishop, 1986). Davidson and Lindsley (1989) adopted an asymmetric model that better approximates the Ca-rich limb of the experimentally determined Fe-free solvus, but as illustrated by Figure 8, deviations from a symmetric solvus are small below 1200 °C and the symmetric approximation produces reasonable fits to all data except for the Ca-rich limb at high

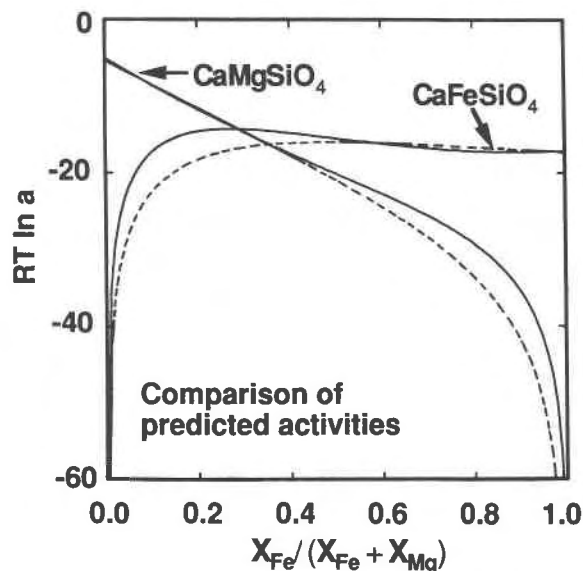


Fig. 9. Calculated values of  $RT \ln a$  for  $\text{CaMgSiO}_4$  and  $\text{CaFeSiO}_4$ , at 900 °C, 1 bar and  $X_{\text{Ca}_2\text{SiO}_4}^{\text{ol}} = 0.01$ . Dashed line = Davidson and Lindsley (1989); solid line = present model.

temperature. Calculated activities of  $\text{CaFeSiO}_4$  for solution of small amounts of Ca in forsteritic olivine and  $\text{CaMgSiO}_4$  in fayalitic olivine do not agree with those from Davidson and Lindsley's (1989) analysis, but the models are otherwise very similar (Fig. 9). Disagreements are attributable almost entirely to different adopted values of  $W_{\text{MgFe}}^{\text{ol}}$ .

It should be noted that asymmetric solvi are not necessarily caused by asymmetric enthalpies of mixing. The apparently asymmetric mixing properties of many solid solutions are the result of symmetric interactions between ordered and disordered components that appear asymmetric only when projected onto the binary bounded by the (macroscopic) compositional end-members (e.g., rhombohedral oxides, Ghiorso, 1990b; spinels, Sack and Ghiorso, 1991). Improved treatment of the asymmetric miscibility gap along the forsterite-monticellite join may not necessarily require third-order (asymmetric) solution terms. Marked asymmetry is manifested only above 1300 °C (Fig. 6) and could be caused by partial disorder of Ca between M1 and M2. In situ X-ray refinements of natural Ca-rich olivines up to 795 °C are consistent with complete order of Ca on M2 (Lager and Meagher, 1978), but lattice parameters of synthetic calcium magnesium olivines suggest small amounts of disorder (Lumpkin et al., 1983; Adams and Bishop, 1985). Small amounts of Ca are known to occupy M1 in calcium iron olivines (Brown, 1980), and substantial Ca enters M1 in calcium cobalt olivines (Kimata and Nishida, 1987). Given the similar cation radii of Co and Mg and in light of the above discussion of the kinetics of order-disorder, it is possible that calcium magnesium olivines are partially disordered at high temperature. If this is the case, calcian olivines can be treated with the ternary version of the model presented

above. Partial disorder at high temperatures would lower the chemical potential of  $\text{CaMgSiO}_4$  relative to the completely ordered standard state, thereby increasing the solubility of Mg in Ca-rich olivines and producing the observed depression of the Ca-rich limb of the solvus. Preliminary calculations indicate that the enthalpy of ordering must be greater than 60 kJ to maintain nearly complete ordering to 800 °C but should be less than about 80 kJ to allow significant (8–10%) Ca on M1 at high temperature (1300–1400 °C).

### Induced ordering

In the present analysis, the enthalpy of Fe-Mg ordering is assumed to be negligible. In multicomponent olivines, however, substantial Fe-Mg ordering may be induced by energetic differences in the way Mg and Fe interact with third components. The equilibrium ordering state for calcic olivines (Eq. A9) depends in part on differences between Ca-Mg and Ca-Fe interaction energies:

$$RT \ln K_d = RT \ln \left( \frac{X_{\text{Fe}}^{\text{M1}} X_{\text{Mg}}^{\text{M2}}}{X_{\text{Mg}}^{\text{M1}} X_{\text{Fe}}^{\text{M2}}} \right) = f [p(W_{\text{CaMg}}^{\text{M2}} - W_{\text{CaFe}}^{\text{M2}})]. \quad (29)$$

Because the difference between  $W_{\text{CaMg}}^{\text{M2}}$  and  $W_{\text{CaFe}}^{\text{M2}}$  is greater than 12 kJ, predicted  $K_d$  values at 2 kbar range from 0.39 at 800 °C to 0.50 at 1200 °C for compositions near the  $\text{CaMgSiO}_4$ - $\text{CaFeSiO}_4$  join.

Induced ordering may also arise from differences in ordering enthalpies between components. For example, the equilibrium Mg-Fe ordering state of Ni-bearing olivines (Eq. A1) depends in part on the difference between Ni-Mg and Ni-Fe ordering energies:

$$RT \ln K_d = RT \ln \left( \frac{X_{\text{Fe}}^{\text{M1}} X_{\text{Mg}}^{\text{M2}}}{X_{\text{Mg}}^{\text{M1}} X_{\text{Fe}}^{\text{M2}}} \right) = f \left[ \frac{(1-q)}{2} \Delta \bar{H}_{\text{EX}}^{\text{FeMg}} + \left( \frac{1+q}{2} \right) (\Delta \bar{H}_{\text{EX}}^{\text{FeNi}} - \Delta \bar{H}_{\text{EX}}^{\text{MgNi}}) \right]. \quad (30)$$

The lack of significant, observed induced Mg-Fe ordering in magnesium iron nickel olivines (Nord et al., 1982) is consistent with the assumption that Ni-Mg and Ni-Fe ordering energies are similar.

### Olivine-alloy equilibria

Compositions of coexisting olivines and Fe-Ni alloys have been determined at 1 bar and 1300 °C (Campbell et al., 1979) and at 5 kbar and 1263 and 1425 °C (Seifert and O'Neill, 1987) and between olivines and liquid Fe-Ni alloys at 20 kbar and 35 kbar at 1600 °C and 1780 °C, respectively. Because olivine-alloy equilibria were not considered during calibration, comparison of predicted and measured compositions of olivines coexisting with Fe-Ni alloys serves as a check on the validity of the pres-

ent model. Predicted olivine-alloy distribution coefficients at a given temperature, alloy composition, and Fe/(Fe + Mg) ratio in olivine, using standard state properties from Appendix 2 and alloy activity coefficients calculated from Larrain (1980), agree within analytical uncertainty ( $2\sigma$ ) with 18 out of 21 experimentally determined olivine-alloy pairs (Fig. 10). The success of these predictions demonstrates the applicability of the olivine solution model and confirms that the combination of assumptions required to construct the model is reasonable.

### SUMMARY AND CONCLUSIONS

Beginning with consideration of cation ordering and the standard state properties of compositional end-members, thermodynamic models are developed to describe substitution of minor divalent cations in ferromagnesian olivines. Calibration of the mixing properties of Ni-bearing olivines from site occupancy data and heterogeneous equilibria indicates negative departures from ideality for  $\text{Ni}_2\text{SiO}_4$  in olivine for compositions relevant to natural olivines. Predictions of the model are in close agreement with experimental olivine-FeNi alloy data. Calibration of Ca-bearing olivines yields predictions for the chemical potential of calcian olivine components that are similar to those of Davidson and Lindsley (1989). Small differences between Davidson and Lindsley's and the present model arise from acceptance here of more strongly positive interactions between Mg and Fe. (Software to calculate chemical potentials and homogeneous equilibrium in nickel magnesium iron and calcium magnesium iron olivines is available by anonymous FTP from internet node [fondue.geo.washington.edu](http://fondue.geo.washington.edu)).

### ACKNOWLEDGMENTS

This contribution was improved by reviews and comments by M.S. Ghiorso, R.O. Sack, D.L. Whitney, V.C. Kress, R.O. Colson, and an anonymous reviewer. The author wishes to thank M.S. Ghiorso and R.O. Sack for particularly helpful discussions. This work was supported by NSF grant EAR-8451694 to M.S. Ghiorso. Computations were aided by an equipment grant from the Digital Equipment Corporation to M.S. Ghiorso.

### REFERENCES CITED

- Adams, G.E., and Bishop, F.C. (1985) An experimental investigation of thermodynamic mixing properties and unit-cell parameters of forsterite-monticellite solid solutions. *American Mineralogist*, 70, 714–722.
- (1986) The olivine-clinopyroxene geobarometer: Experimental results in the  $\text{CaO-FeO-MgO-SiO}_2$  system. *Contributions to Mineralogy and Petrology*, 94, 230–237.
- Aikawa, N., Kumazawa, M., and Tokanami, M. (1985) Temperature dependence of intersite distribution of Mg and Fe in olivine and the associated change of lattice parameters. *Physics and Chemistry of Minerals*, 12, 1–8.
- Annersten, H., and Filippidis, A. (1984) Cation ordering in Ni-Fe olivines: Reply. *American Mineralogist*, 69, 164.
- Annersten, H., Ericsson, T., and Filippidis, A. (1982) Cation ordering in Ni-Fe olivines. *American Mineralogist*, 67, 1212–1217.
- Anovitz, L.M., Essene, E.J., and Dunham, W.R. (1988) Order-disorder experiments on orthopyroxenes: Implications for the orthopyroxene geospeedometer. *American Mineralogist*, 73, 1060–1073.
- Bass, J.D., Weidner, D.J., Hamaya, N., Ozima, M., and Akimoto, S.

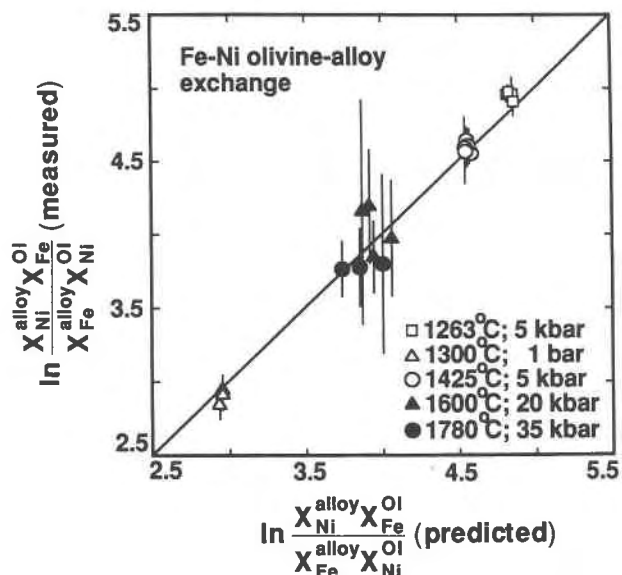


Fig. 10. Predicted-measured olivine-alloy distribution coefficient. Data of 1300 °C from Campbell et al. (1979); other data from Seifert et al. (1988). Alloys at 1600 and 1780 °C are liquid (filled symbols); other alloys are crystalline (open symbols). Olivines and alloys from Seifert et al. (1988) contain up to 0.08 mol% and 2.5 mol% cobalt components, respectively. Error bar represents analytical uncertainty of 2 s.d.

- (1984) Elasticity of the olivine and spinel polymorphs of  $\text{Ni}_2\text{SiO}_4$ . *Physics and Chemistry of Minerals*, 10, 261–272.
- Berman, R.G. (1988) Internally-consistent thermodynamic data for minerals in the system  $\text{Na}_2\text{O-K}_2\text{O-CaO-MgO-FeO-Fe}_2\text{O}_3\text{-Al}_2\text{O}_3\text{-SiO}_2\text{-TiO}_2\text{-H}_2\text{O-CO}_2$ . *Journal of Petrology*, 29, 445–522.
- Berman, R.G., and Brown, T.H. (1985) Heat capacity of mineral in the system  $\text{Na}_2\text{O-K}_2\text{O-CaO-MgO-FeO-Fe}_2\text{O}_3\text{-Al}_2\text{O}_3\text{-SiO}_2\text{-TiO}_2\text{-H}_2\text{O-CO}_2$ : Representation, estimation, and high temperature extrapolation. *Contributions to Mineralogy and Petrology*, 89, 168–183.
- Birch, F. (1966) Compressibility; elastic constants. *Geological Society of America Memoir*, 97, 97–174.
- Bish, D.L. (1981) Cation ordering in synthetic and natural Ni-Mg olivine. *American Mineralogist*, 66, 770–776.
- Boström, D. (1987) Single-crystal X-ray diffraction studies of synthetic Ni-Mg olivine solid solutions. *American Mineralogist*, 72, 965–972.
- Boström, D., and Rosén, E. (1988) Determination of activity-composition in (Ni,Mg) $_2$ SiO $_4$  solid solution at 1200–1600 K by solid state emf measurements. *Acta Chemica Scandinavica*, A42, 149–155.
- Bragg, W.L., and Williams, E.J. (1934) The effect of thermal agitation on atomic arrangement in alloys. *Proceedings of the Royal Society of London A*, 145, 699–730.
- Brown, G.E. (1980) Olivines and silicate spinels. In *Mineralogical Society of America Reviews in Mineralogy*, 5, 275–381.
- Campbell, F.E., and Roeder, P. (1968) The stability of olivine and pyroxene in the Ni-Mg-Si-O system. *American Mineralogist*, 53, 257–268.
- Campbell, I.H., Naldrett, A.J., and Roeder, P. (1979) Nickel activity in silicate liquids: Some preliminary results. *Canadian Mineralogist*, 17, 495–505.
- Chase, M.W., Curnett, J.L., Hu, A.T., Prophet, H., Syverud, A.N., and Walker, L.C. (1974) JANAF thermochemical tables. *Journal of Physics and Chemistry Reference Data*, 3, 311–480.
- Clendenen, R.L., and Drickamer, H.G. (1966) Lattice parameters of nine oxides and sulfides as a function of pressure. *Journal of Chemical Physics*, 44, 4223–4228.
- Colson, R.O., McKay, G.A., and Taylor, L.A. (1988) Temperature and

- compositional dependence of trace element partitioning: Olivine/melt and orthopyroxene/melt. *Geochimica et Cosmochimica Acta*, 52, 539–553.
- (1989) Partitioning data pertaining to Fe-Mg ordering around trace cations in olivine and low-Ca pyroxene. *Contributions to Mineralogy and Petrology*, 102, 242–246.
- Darken, L.S., and Gurry, R.W. (1953) *Physical chemistry of metals*. McGraw Hill, New York.
- Davidson, P.M. (1985) Thermodynamic analysis of quadrilateral pyroxenes. Part I: Derivation of the ternary nonconvergent site-disorder model. *Contributions to Mineralogy and Petrology*, 91, 383–389.
- Davidson, P.M., and Lindsley, D.H. (1989) Thermodynamic analysis of pyroxene-olivine-quartz equilibria in the system CaO-MgO-FeO-SiO<sub>2</sub>. *American Mineralogist*, 74, 18–30.
- Davidson, P.M., and Mukhopadhyay, D.K. (1984) Ca-Fe-Mg olivines: Phase relations and a solution model. *Contributions to Mineralogy and Petrology*, 86, 256–263.
- Davies, P.K., and Navrotsky, A. (1981) Thermodynamics of solid solution formation in NiO-MgO and NiO-ZnO. *Journal of Solid State Chemistry*, 38, 264–276.
- Davies, P.K., Mackinnon, I.D.R., and Navrotsky, A. (1980) Ordering in NiO-MgO solid solutions. *Eos*, 61, 1148.
- Doyle, C.D., and Naldrett, A.J. (1987) Ideal mixing of divalent cations in mafic magma. II. The solution of NiO and the partitioning of nickel between coexisting olivine and liquid. *Geochimica et Cosmochimica Acta*, 51, 213–219.
- Evans, L.G., and Muan, A. (1971) Activity-composition relations in solid solutions and stabilities of end-member compounds in the system MgO-NiO-TiO<sub>2</sub> in contact with metallic nickel at 1400 °C. *Thermochimica Acta*, 2, 121–134.
- Fleet, M.E. (1989) Activity coefficients for FeS and NiS in monosulfide liquid and NiSi<sub>1.7</sub>O<sub>2</sub> in olivine from sulfide-silicate equilibria. *Geochimica et Cosmochimica Acta*, 53, 791–796.
- Fleet, M.E., and MacRae, N.D. (1988) Partition of Ni between olivine and sulfide: Equilibria with sulfide-oxide liquids. *Contributions to Mineralogy and Petrology*, 100, 462–469.
- Ghiorso, M.S. (1985) Chemical mass transfer in magmatic processes. I. Thermodynamic relations and numerical algorithms. *Contributions to Mineralogy and Petrology*, 90, 107–120.
- (1990a) A note on the application of the Darken equation to mineral solid-solutions with variable degrees of order-disorder. *American Mineralogist*, 75, 539–543.
- (1990b) Thermodynamic properties of hematite-ilmenite-geikelite solid solutions. *Contributions to Mineralogy and Petrology*, 104, 645–667.
- Ghose, S., and Wan, C. (1974) Strong site preference of Co<sup>2+</sup> in olivine, Co<sub>1-10</sub>Mg<sub>90-90</sub>SiO<sub>4</sub>. *Contributions to Mineralogy and Petrology*, 47, 131–140.
- Griffen, W.L., Cousens, D.R., Ryan, C.G., Sie, S.H., and Suter, G.F. (1989) Ni in chrome pyrope garnets: A new geothermometer. *Contributions to Mineralogy and Petrology*, 103, 199–202.
- Hahn, W.C., and Muan, A. (1961) Activity measurements in oxide solid solutions in the systems NiO-MgO and NiO-MnO in the temperature interval 1100–1300 °C. *Journal of Physical Chemistry of Solids*, 19, 338–348.
- Hakli, T.A., and Wright, T.L. (1967) The fractionation of nickel between olivine and augite as a geothermometer. *Geochimica et Cosmochimica Acta*, 31, 877–884.
- Hart, S.R., and Davis, K.E. (1978) Nickel partitioning between olivine and silicate melt. *Earth and Planetary Science Letters*, 40, 203–219.
- Hemingway, B.S. (1990) Thermodynamic properties for bunsenite, NiO, magnetite, Fe<sub>3</sub>O<sub>4</sub>, and hematite, Fe<sub>2</sub>O<sub>3</sub>, with comments on selected oxygen buffer reactions. *American Mineralogist*, 75, 781–790.
- Hu, X., Langer, K., and Boström, D. (1990) Polarized electronic absorption spectra and Ni-Mg partitioning in olivines (Mg<sub>1-x</sub>Ni<sub>x</sub>)[SiO<sub>4</sub>]. *European Journal of Mineralogy*, 2, 29–41.
- Jones, J.H., and Drake, M.J. (1986) Geochemical constraints on core formation in the Earth. *Nature*, 322, 221–228.
- Jurewicz, A.J.G., and Watson, E.B. (1988) Cations in olivine, Part 1: Calcium partitioning and calcium-magnesium distribution between olivines and coexisting melts, and petrologic applications. *Contributions to Mineralogy and Petrology*, 99, 176–185.
- Kawasaki, T., and Matsui, Y. (1983) Thermodynamic analyses of equilibria involving olivine, orthopyroxene, and garnet. *Geochimica et Cosmochimica Acta*, 47, 1661–1679.
- Kimata, M., and Nishida, N. (1987) The crystal structure of Co-monticellite Ca<sub>1.25</sub>Co<sub>0.745</sub>SiO<sub>4</sub> and its significance as a solid solution crystal. *Neues Jahrbuch für Mineralogie Monatshefte*, H4, 160–170.
- Kinzler, R.J., Grove, T.L., and Recca, S.I. (1990) An experimental study on the effect of temperature and composition on the partitioning of nickel between olivine and silicate melt. *Geochimica et Cosmochimica Acta*, 54, 1255–1265.
- Lager, G.A., and Meagher, E.P. (1978) High temperature study of six olivines. *American Mineralogist*, 63, 365–377.
- Larrain, J.M. (1980) High temperature thermodynamic properties of iron-nickel alloys. *CALPHAD*, 4, 155–171.
- Leeman, W.P., and Lindstrom, D.J. (1978) Partitioning of Ni<sup>2+</sup> between basaltic and synthetic melts and olivines—an experimental study. *Geochimica et Cosmochimica Acta*, 42, 801–816.
- Levitskii, V.A., Golovanova, Y.G., Popov, S.G., and Chentsov, V.N. (1975) Thermodynamics of binary oxide systems. Thermodynamic properties of nickel orthosilicate. *Russian Journal of Physical Chemistry*, 36, 460–461.
- Lumpkin, G.R., Ribbe, P.H., and Lumpkin, N.E. (1983) Composition, order-disorder and lattice parameters of olivines: Determinative methods for Mg-Mn and Mg-Ca silicate olivines. *American Mineralogist*, 68, 1174–1182.
- Mah, A.D., and Pankratz, L.B. (1976) Contributions to the data on theoretical metallurgy XVI. Thermodynamic properties of nickel and its inorganic compounds. *U.S. Bureau of Mines Bulletin*, 668, 1–125.
- Matsui, Y., and Syono, Y. (1968) Unit cell dimensions of some synthetic olivine group solid solutions. *Geochemical Journal*, 2, 51–59.
- McCormick, T.C., Smyth, J.R., and Lofgren, G.E. (1987) Site occupancies of minor elements in synthetic olivines as determined by channeling-enhanced X-ray emission. *Physics and Chemistry of Minerals*, 14, 368–372.
- Motoyama, T., and Matsumoto, T. (1989) The crystal structures and the cation distributions of Mg and Fe in natural olivines. *Mineralogical Journal*, 14, 338–350.
- Mukhopadhyay, D.K., and Lindsley, D.H. (1983) Phase relations in the join kirschsteinite (CaFeSiO<sub>4</sub>)–fayalite (Fe<sub>2</sub>SiO<sub>4</sub>). *American Mineralogist*, 68, 1089–1094.
- Navrotsky, A. (1971) Thermodynamics of formation of the silicates and germanates of some divalent transition metals and of magnesium. *Journal of Inorganic and Nuclear Chemistry*, 33, 4035–4050.
- Nord, A.G., Annersten, H., and Filippidis, A. (1982) The cation distribution in synthetic Mg-Fe-Ni olivines. *American Mineralogist*, 67, 1206–1211.
- O'Neill, H.St.C. (1987) Free energies of formation of NiO, CoO, Ni<sub>2</sub>SiO<sub>4</sub>, and Co<sub>2</sub>SiO<sub>4</sub>. *American Mineralogist*, 72, 280–291.
- Ottonello, G., and Morlotti, R. (1987) Thermodynamics of the (nickel + magnesium) olivine solid solution. *Journal of Chemical Thermodynamics*, 19, 809–818.
- Ottonello, G., Della Giusta, A., and Molin, G.M. (1989) Cation ordering in Ni-Mg olivines. *American Mineralogist*, 74, 411–421.
- Ottonello, G., Princivalle, F., and Della Giusta, A. (1990) Temperature, composition, and f<sub>O<sub>2</sub></sub> effects on intersite distribution of Mg and Fe<sup>2+</sup> in olivines: Experimental evidence and theoretical interpretation. *Physics and Chemistry of Minerals*, 17, 301–312.
- Ozima, M. (1976) Growth of nickel olivine single crystals by the flux method. *Journal of Crystal Growth*, 33, 193–195.
- Paulsson, H. (1982) Activities in NiO in (Ni,Mg)O solid solutions. *Chemica Scripta*, 19, 116–117.
- Phillips, B., Hutta, J.J., and Warshaw, I. (1963) Phase equilibria in the system NiO-Al<sub>2</sub>O<sub>3</sub>-SiO<sub>2</sub>. *Journal of the American Ceramic Society*, 46, 579–583.
- Podvin, P. (1988) Ni-Mg partitioning between synthetic olivines and orthopyroxenes: Application to geothermometry. *American Mineralogist*, 73, 274–280.
- Rajamani, V., Brown, G.E., and Prewitt, C.T. (1975) Cation ordering in Ni-Mg olivine. *American Mineralogist*, 60, 292–299.
- Ringwood, A.E. (1986) Terrestrial origin of the Moon. *Nature*, 322, 323–328.
- Ringwood, A.E., and Seifert, S. (1986) Nickel-cobalt abundance system-

atics and their bearing on lunar origin. In W.K. Hartmann, R.J. Phillips, and G.J. Taylor, Eds., *Origin of the Moon*, p. 249–278. Lunar and Planetary Institute, Houston, Texas.

- Robie, R.A., Hemingway, B.S., and Fischer, J.R. (1979) Thermodynamic properties of minerals and related substances at 298.15 K and 1 bar ( $10^5$  Pascals) pressure and at higher temperatures. United States Geological Survey Bulletin, 1452, 456 p.
- Robie, R.A., Hemingway, B.S., Ito, J., and Krupka, K.M. (1984) Heat capacity and entropy of  $\text{Ni}_2\text{SiO}_4$  olivine from 5 to 1000 K and heat capacity of  $\text{Co}_2\text{SiO}_4$  from 360 to 1000 K. *American Mineralogist*, 69, 1096–1101.
- Rog, G., and Borchardt, G. (1984) Thermodynamics of nickel orthosilicate. *Journal of Chemical Thermodynamics*, 16, 1103–1105.
- Sack, R.O. (1980) Some constraints on the thermodynamic mixing properties of Fe-Mg orthopyroxenes and olivines. *Contributions to Mineralogy and Petrology*, 71, 257–269.
- Sack, R.O., and Ghiorso, M.S. (1989) Importance of considerations of mixing properties in establishing an internally consistent thermodynamic database: Thermochemistry of minerals in the system  $\text{Mg}_2\text{SiO}_4$ - $\text{Fe}_2\text{SiO}_4$ - $\text{SiO}_2$ . *Contributions to Mineralogy and Petrology*, 102, 41–68.
- (1991) An internally consistent model for the thermodynamic properties of Fe-Mg-titanomagnetite-aluminate spinels. *Contributions to Mineralogy and Petrology*, 106, 474–505.
- Seifert, S., and O'Neill, H.S.C. (1987) Experimental determination of activity-composition relations in  $\text{Ni}_2\text{SiO}_4$ - $\text{Mg}_2\text{SiO}_4$  and  $\text{Co}_2\text{SiO}_4$ - $\text{Mg}_2\text{SiO}_4$  olivine solid solutions at 1200 K and 0.1 MPa and 1573 K and 0.5 GPa. *Geochimica et Cosmochimica Acta*, 51, 97–104.
- Seifert, S., O'Neill, H.S.C., and Brey, G. (1988) The partitioning of Fe, Ni and Co between olivine, metal and basaltic liquid: An experimental and thermodynamic investigation with application to the composition of the lunar core. *Geochimica et Cosmochimica Acta*, 52, 603–616.
- Simpkin, T., and Smith, J.V. (1970) Minor element distribution in olivine. *Journal of Geology*, 78, 304–325.
- Skinner, B.J. (1966) Thermal expansion. *Geological Society of America Memoir*, 97, 75–96.
- Smyth, J.R., and Taftø, J. (1982) Major and minor site occupancies in heated natural forsterite. *Geophysical Research Letters*, 9, 1113–1116.
- Stosch, H. (1981) Sc, Cr, Co, and Ni partitioning between minerals from spinel peridotite xenoliths. *Contributions to Mineralogy and Petrology*, 78, 166–174.
- Takahashi, E. (1978) Partitioning of  $\text{Ni}^{2+}$ ,  $\text{Co}^{2+}$ ,  $\text{Fe}^{2+}$ ,  $\text{Mn}^{2+}$ , and  $\text{Mg}^{2+}$  between olivine and silicate melts: Compositional dependences of partition coefficient. *Geochimica et Cosmochimica Acta*, 42, 1829–1844.
- Taylor, R.W., and Schmalzried, J. (1964) The free energy of formation of some titanites, silicates and magnesium aluminate from measurements made with galvanic cells involving solid electrolytes. *Journal of Physical Chemistry*, 68, 2444–2449.
- Thompson, J.B., Jr. (1969) Chemical reactions in crystals. *American Mineralogist*, 54, 341–375.
- (1970) Chemical reactions in crystals: Corrections and clarification. *American Mineralogist*, 55, 528–532.
- Touloukian, Y.S. (1967) Thermophysical properties of high temperature solid materials. Macmillan, New York.
- Vokurka, K., and Rieder, M. (1987) Thermal expansion and excess volumes of synthetic olivines on the  $\text{Mg}_2\text{SiO}_4$ - $\text{Ni}_2\text{SiO}_4$  join. *Neues Jahrbuch für Mineralogie Monatshefte*, H3, 97–106.
- Watanabe, S. (1971) Densities and viscosities of iron, cobalt and Fe-Co alloys in liquid state. *Transactions of the Japanese Institute of Metals*, 12, 17–22.
- Watanabe, S., Amatatu, M., and Saito, T. (1971) Densities of Fe-Ni, Co-Ni, Co-Mo and Co-W alloys in liquid state. *Transactions of the Japanese Institute of Metals*, 12, 337–342.
- Williams, R.J. (1972) Activity-composition relations in the fayalite-forsterite solid solution between 900° and 1300° at low pressures. *Earth and Planetary Science Letters*, 15, 296–300.
- Wood, B.J., and Nicholls, J. (1978) The thermodynamic properties of reciprocal solid solutions. *Contributions to Mineralogy and Petrology*, 66, 389–400.

## APPENDIX 1. EQUATIONS FOR EQUILIBRIUM ORDERING STATE AND EXCHANGE CHEMICAL POTENTIALS

### Nickel magnesium iron olivines

$$\left(\frac{\partial \bar{G}}{\partial s}\right)_{q,r,t} = 0 = \frac{1}{2} \left[ RT \ln \left( \frac{X_{\text{Fe}}^{\text{M2}} X_{\text{Mg}}^{\text{M1}}}{X_{\text{Fe}}^{\text{M1}} X_{\text{Mg}}^{\text{M2}}} \right) + \frac{(1-q)}{2} \Delta \bar{G}_{\text{EX}}^{\text{FeMg}} \right. \\ + \frac{(1+q)}{2} (\Delta \bar{G}_{\text{EX}}^{\text{FeNi}} - W_{\text{FeNi}}^{\text{M1}} + W_{\text{FeNi}}^{\text{M2}} \\ - \Delta \bar{G}_{\text{EX}}^{\text{MgNi}} + W_{\text{MgNi}}^{\text{M1}} - W_{\text{MgNi}}^{\text{M2}}) \\ + \frac{(1+q+2r)}{2} (W_{\text{FeMg}}^{\text{M1}} - W_{\text{FeMg}}^{\text{M2}}) \\ + \frac{(2s-t)}{2} (\Delta \bar{G}_X^{\text{FeMg}} - W_{\text{FeMg}}^{\text{M1}} - W_{\text{FeMg}}^{\text{M2}}) \\ + \frac{t}{2} (\Delta \bar{G}_X^{\text{FeNi}} - W_{\text{FeNi}}^{\text{M1}} - W_{\text{FeNi}}^{\text{M2}} \\ \left. - \Delta \bar{G}_X^{\text{MgNi}} - W_{\text{MgNi}}^{\text{M1}} - W_{\text{MgNi}}^{\text{M2}}) \right] \quad (\text{A1})$$

$$\left(\frac{\partial \bar{G}}{\partial t}\right)_{q,r,s} = 0 = \frac{1}{2} \left[ RT \ln \left( \frac{X_{\text{Ni}}^{\text{M1}} X_{\text{Mg}}^{\text{M2}}}{X_{\text{Ni}}^{\text{M2}} X_{\text{Mg}}^{\text{M1}}} \right) + \frac{(1-r)}{2} \Delta \bar{G}_{\text{EX}}^{\text{MgNi}} \right. \\ + \frac{(1+r)}{2} (\Delta \bar{G}_{\text{EX}}^{\text{FeNi}} + W_{\text{FeNi}}^{\text{M1}} - W_{\text{FeNi}}^{\text{M2}} \\ - \Delta \bar{G}_{\text{EX}}^{\text{FeMg}} - W_{\text{FeMg}}^{\text{M1}} + W_{\text{FeMg}}^{\text{M2}}) \\ + \frac{(1+2q+r)}{2} (W_{\text{MgNi}}^{\text{M2}} - W_{\text{MgNi}}^{\text{M1}}) \\ + \frac{(2t-s)}{2} (\Delta \bar{G}_X^{\text{MgNi}} - W_{\text{MgNi}}^{\text{M1}} - W_{\text{MgNi}}^{\text{M2}}) \\ + \frac{s}{2} (\Delta \bar{G}_X^{\text{FeNi}} - W_{\text{FeNi}}^{\text{M1}} - W_{\text{FeNi}}^{\text{M2}} \\ \left. - \Delta \bar{G}_X^{\text{FeMg}} - W_{\text{FeMg}}^{\text{M1}} - W_{\text{FeMg}}^{\text{M2}}) \right] \quad (\text{A2})$$

$$\mu_{\text{NiMg-1}} = \frac{1}{2} \left[ \bar{G}_{\text{Ni}_2\text{SiO}_4}^0 - \bar{G}_{\text{Mg}_2\text{SiO}_4}^0 + RT \ln \left( \frac{X_{\text{Ni}}^{\text{M1}} X_{\text{Ni}}^{\text{M2}}}{X_{\text{Mg}}^{\text{M1}} X_{\text{Mg}}^{\text{M2}}} \right) \right] \\ + \frac{(1+r-2q)}{4} (\Delta \bar{G}_X^{\text{MgNi}} + W_{\text{MgNi}}^{\text{M1}} + W_{\text{MgNi}}^{\text{M2}}) \\ + \frac{t}{2} (W_{\text{MgNi}}^{\text{M2}} - W_{\text{MgNi}}^{\text{M1}}) \\ + \frac{(1+r)}{4} [(\Delta \bar{G}_X^{\text{FeNi}} + W_{\text{FeNi}}^{\text{M1}} + W_{\text{FeNi}}^{\text{M2}} \\ - (\Delta \bar{G}_X^{\text{FeMg}} + W_{\text{FeMg}}^{\text{M1}} + W_{\text{FeMg}}^{\text{M2}})] \\ + \frac{s}{4} [(\Delta \bar{G}_{\text{EX}}^{\text{FeNi}} - W_{\text{FeNi}}^{\text{M1}} + W_{\text{FeNi}}^{\text{M2}}) \\ - (\Delta \bar{G}_{\text{EX}}^{\text{MgNi}} - W_{\text{MgNi}}^{\text{M1}} + W_{\text{MgNi}}^{\text{M2}}) \\ - (\Delta \bar{G}_{\text{EX}}^{\text{FeMg}} - W_{\text{FeMg}}^{\text{M1}} + W_{\text{FeMg}}^{\text{M2}})] \quad (\text{A3})$$



$$\begin{aligned} \mu_{\text{NiFe}_{-1}} = & \frac{1}{2} \left[ \bar{G}_{\text{Ni}_2\text{SiO}_4}^0 - \bar{G}_{\text{Fe}_2\text{SiO}_4}^0 + RT \ln \left( \frac{X_{\text{Ni}}^{\text{M1}} X_{\text{Ni}}^{\text{M2}}}{X_{\text{Fe}}^{\text{M1}} X_{\text{Fe}}^{\text{M2}}} \right) \right] \\ & + \left( \frac{r-q}{2} \right) (\Delta \bar{G}_X^{\text{FeNi}} + W_{\text{FeNi}}^{\text{M1}} + W_{\text{FeNi}}^{\text{M2}}) \\ & + \frac{s+t}{4} (W_{\text{FeNi}}^{\text{M2}} - W_{\text{FeNi}}^{\text{M1}}) \\ & + \frac{(r+q)}{4} [(\Delta \bar{G}_X^{\text{FeMg}} + W_{\text{FeMg}}^{\text{M1}} + W_{\text{FeMg}}^{\text{M2}}) \\ & \quad - (\Delta \bar{G}_X^{\text{MgNi}} + W_{\text{MgNi}}^{\text{M1}} + W_{\text{MgNi}}^{\text{M2}})] \\ & + \frac{(t-s)}{4} [(\Delta \bar{G}_{\text{EX}}^{\text{FeMg}} + W_{\text{FeMg}}^{\text{M1}} - W_{\text{FeMg}}^{\text{M2}}) \\ & \quad + (\Delta \bar{G}_{\text{EX}}^{\text{MgNi}} - W_{\text{MgNi}}^{\text{M1}} + W_{\text{MgNi}}^{\text{M2}}) - \Delta \bar{G}_{\text{EX}}^{\text{FeNi}}] \quad (\text{A4}) \end{aligned}$$

$$\begin{aligned} \mu_{\text{MgFe}_{-1}} = & \frac{1}{2} \left[ \bar{G}_{\text{Mg}_2\text{SiO}_4}^0 - \bar{G}_{\text{Fe}_2\text{SiO}_4}^0 + RT \ln \left( \frac{X_{\text{Mg}}^{\text{M1}} X_{\text{Mg}}^{\text{M2}}}{X_{\text{Fe}}^{\text{M1}} X_{\text{Fe}}^{\text{M2}}} \right) \right] \\ & + \frac{(2r-q-1)}{4} (\Delta \bar{G}_X^{\text{MgFe}} + W_{\text{MgFe}}^{\text{M1}} + W_{\text{MgFe}}^{\text{M2}}) \\ & + \frac{s}{2} (W_{\text{MgFe}}^{\text{M2}} - W_{\text{MgFe}}^{\text{M1}}) \\ & + \frac{(1+q)}{4} [(\Delta \bar{G}_X^{\text{MgNi}} + W_{\text{MgNi}}^{\text{M1}} + W_{\text{MgNi}}^{\text{M2}}) \\ & \quad - (\Delta \bar{G}_X^{\text{FeNi}} + W_{\text{FeNi}}^{\text{M1}} + W_{\text{FeNi}}^{\text{M2}})] \\ & + \frac{t}{4} [(\Delta \bar{G}_{\text{EX}}^{\text{MgNi}} + W_{\text{MgNi}}^{\text{M1}} - W_{\text{MgNi}}^{\text{M2}}) \\ & \quad - (\Delta \bar{G}_{\text{EX}}^{\text{FeNi}} + W_{\text{FeNi}}^{\text{M1}} - W_{\text{FeNi}}^{\text{M2}}) \\ & \quad + (\Delta \bar{G}_{\text{EX}}^{\text{FeMg}} + W_{\text{FeMg}}^{\text{M1}} - W_{\text{FeMg}}^{\text{M2}})] \quad (\text{A5}) \end{aligned}$$

### Calcium magnesium iron olivines

$$\begin{aligned} \left( \frac{\partial \bar{G}}{\partial s} \right)_{p,r} = & 0 = \frac{1}{2} \left[ RT \ln \left( \frac{X_{\text{Fe}}^{\text{M2}} X_{\text{Mg}}^{\text{M1}}}{X_{\text{Fe}}^{\text{M1}} X_{\text{Mg}}^{\text{M2}}} \right) + \frac{(2-p)}{2} \Delta \bar{G}_{\text{EX}}^{\text{FeMg}} \right. \\ & + p \left( \frac{\bar{F}^0}{2} - W_{\text{CaFe}}^{\text{M2}} - W_{\text{CaMg}}^{\text{M2}} \right) \\ & + \frac{(2r+p)}{2} (W_{\text{FeMg}}^{\text{M1}} - W_{\text{FeMg}}^{\text{M2}}) \\ & \left. + \frac{(2s+p)}{2} (\Delta \bar{G}_X^{\text{FeMg}} - W_{\text{FeMg}}^{\text{M1}} - W_{\text{FeMg}}^{\text{M2}}) \right] \quad (\text{A6}) \end{aligned}$$

$$\begin{aligned} \mu_{\text{CaMgSiO}_4} = & \bar{G}_{\text{CaMgSiO}_4}^0 + RT \ln (X_{\text{Ca}}^{\text{M2}} X_{\text{Mg}}^{\text{M1}}) \\ & + (p-1) \left[ \frac{(r-s+1)}{4} (\Delta \bar{G}_X^{\text{FeMg}} - \Delta \bar{G}_{\text{EX}}^{\text{FeMg}} + \bar{F}^0) \right. \\ & \quad + (p-1) W_{\text{CaMg}}^{\text{M2}} \\ & \quad \left. + \frac{(s+r+1)}{2} (W_{\text{CaMg}}^{\text{M2}} + W_{\text{FeMg}}^{\text{M2}} - W_{\text{CaFe}}^{\text{M2}}) \right] \\ & + \frac{(r+1)^2}{4} (\Delta \bar{G}_X^{\text{FeMg}} + W_{\text{FeMg}}^{\text{M1}} + W_{\text{FeMg}}^{\text{M2}}) \\ & + \frac{s(r+1)}{2} (W_{\text{FeMg}}^{\text{M2}} - W_{\text{FeMg}}^{\text{M1}}) \end{aligned}$$

$$- \frac{s^2}{4} (\Delta \bar{G}_X^{\text{FeMg}} - W_{\text{FeMg}}^{\text{M1}} - W_{\text{FeMg}}^{\text{M2}}) \quad (\text{A7})$$

$$\begin{aligned} \mu_{\text{CaFeSiO}_4} = & \bar{G}_{\text{CaMgSiO}_4}^0 + \frac{\bar{G}_{\text{FeFeSiO}_4}^0 - \bar{G}_{\text{MgMgSiO}_4}^0 - \bar{F}^0}{2} \\ & + RT \ln (X_{\text{Ca}}^{\text{M2}} X_{\text{Fe}}^{\text{M1}}) \\ & + (p-1) \left[ \frac{(r-s-1)}{4} (\Delta \bar{G}_X^{\text{FeMg}} - \Delta \bar{G}_{\text{EX}}^{\text{FeMg}} + \bar{F}^0) \right. \\ & \quad + (p-1) W_{\text{CaMg}}^{\text{M2}} \\ & \quad \left. + \frac{(s+r+1)}{2} W_{\text{CaMg}}^{\text{M2}} + W_{\text{FeMg}}^{\text{M2}} - W_{\text{CaFe}}^{\text{M2}} \right] \\ & + \frac{r^2}{4} (\Delta \bar{G}_X^{\text{FeMg}} + W_{\text{FeMg}}^{\text{M1}} + W_{\text{FeMg}}^{\text{M2}}) \\ & + \frac{s(1+s)}{2} (W_{\text{FeMg}}^{\text{M2}} - W_{\text{FeMg}}^{\text{M1}}) \\ & - \frac{(s+1)^2}{4} (\Delta \bar{G}_X^{\text{FeMg}} - W_{\text{FeMg}}^{\text{M1}} - W_{\text{FeMg}}^{\text{M2}}) \quad (\text{A8}) \end{aligned}$$

$$\begin{aligned} \mu_{\text{MgFe}_{-1}} = & \frac{1}{2} \left[ \bar{G}_{\text{Mg}_2\text{SiO}_4}^0 - \bar{G}_{\text{Fe}_2\text{SiO}_4}^0 + RT \ln \left( \frac{X_{\text{Mg}}^{\text{M2}} X_{\text{Mg}}^{\text{M1}}}{X_{\text{Fe}}^{\text{M2}} X_{\text{Fe}}^{\text{M1}}} \right) \right] \\ & + \frac{r}{2} (\Delta \bar{G}_X^{\text{FeMg}} + W_{\text{FeMg}}^{\text{M1}} + W_{\text{FeMg}}^{\text{M2}}) \\ & + \frac{s}{2} (W_{\text{FeMg}}^{\text{M2}} - W_{\text{FeMg}}^{\text{M1}}) \\ & + p \left[ \frac{1}{2} (W_{\text{CaMg}}^{\text{M2}} + W_{\text{FeMg}}^{\text{M2}} - W_{\text{CaFe}}^{\text{M2}}) \right. \\ & \left. + \frac{1}{4} (\Delta \bar{G}_X^{\text{FeMg}} - \Delta \bar{G}_{\text{EX}}^{\text{FeMg}} + \bar{F}^0) \right] \quad (\text{A9}) \end{aligned}$$

## APPENDIX 2. SOURCES OF STANDARD STATE THERMODYNAMIC DATA

Evaluation of olivine-oxide and olivine-alloy equilibria requires selection of thermodynamic properties for MgO, NiO, Fe, and Ni metal. The properties of MgO have been taken from Berman (1988). The entropy, heat capacity, and enthalpy of formation of NiO at 1 bar is from Hemingway (1990). The partial molar volume of NiO is from Robie et al. (1979), and thermal expansivity and compressibility are from Touloukian (1967) and Clendenen and Drickamer (1966).

The enthalpy, entropy, and heat capacity of  $\gamma$ -Fe, liquid Fe, liquid Ni, and the entropy of Ni metal are from JANAF (Chase et al., 1974). Enthalpy and heat capacity of Ni metal are from Mah and Pankratz (1976). The partial molar volume of  $\gamma$ -Fe at the reference temperature (298.15 K) is taken as 0.6842 J/bar, calculated from the partial molar of  $\alpha$ -Fe (Touloukian, 1967) adjusted for the change in volume of the  $\alpha$ - $\gamma$  transition and thermal expansion reported by Skinner (1966). Thermal expansivities and compressibilities of solid metals are from Skinner (1966) and Birch (1966), respectively. The thermal expansivities of liquid Fe and liquid Ni are from Watanabe (1971) and Watanabe et al. (1971).